

Review

# Enhancement of Photocatalytic Antimicrobial Performance via Generation and Diffusion of ROS

Xiaojuan Bai<sup>1,2,\*</sup>, Yihan Cao<sup>1</sup>, Bowen Zhu<sup>1</sup>, Rujiao Liu<sup>1</sup>, Jiaqian Dong<sup>1</sup>, and Hua Yang<sup>1</sup><sup>1</sup> Key Laboratory of Urban Stormwater System and Water Environment, Ministry of Education, Beijing University of Civil Engineering and Architecture, Beijing 100044, China<sup>2</sup> Beijing Energy Conservation & Sustainable Urban and Rural Development Provincial and Ministry Co-construction Collaboration Innovation Center, Beijing University of Civil Engineering and Architecture, Beijing 100044, China\* Correspondence: [baixiaojuan@bucea.edu.cn](mailto:baixiaojuan@bucea.edu.cn)

Received: 8 June 2024; Revised: 8 August 2024; Accepted: 20 August 2024; Published: 20 September 2024

**Abstract:** The increasing prevalence of antibiotic-resistant infections globally emphasizes the urgent need for effective antimicrobial strategies. Photocatalysts, known for their efficiency, broad-spectrum activity, and environmental benefits, present a promising alternative. With the development of natural solar light driven photocatalysts, the antimicrobial and bactericidal range has been further extended. Photocatalytic materials can be activated by various light wavelengths to generate reactive oxygen species (ROS), which can effectively eliminate a wide range of pathogenic microorganisms including bacteria, fungi, and protozoa. However, the limited optical response range, suboptimal bandgap, and slow electron cycling limit the efficient generation of ROS, resulting in lower sterilization efficiency of photocatalytic antimicrobials. Additionally, the short half-life and limited migration distance of ROS restrict their antimicrobial activity. This review focuses on the process and mechanism of ROS generation in photocatalytic reactions, and highlighting the recent advances in the typical photocatalysts. We also explore strategies to enhance ROS diffusion and utilization, including morphology control, noble metal deposition, doping, co-catalyst loading, vacancy introduction, surface functionalization, and heterojunction construction. These strategies aim to increase the efficiency of ROS generation and prolong their activity, thereby enhancing the overall antimicrobial effectiveness. Thereafter, the review presents state-of-the-art applications of photocatalysts in water purification, medical coatings, and air disinfection. Furthermore, it explores key challenges and opportunities that may drive future innovations and advancements in photocatalytic antimicrobial applications, aiming to develop more effective and sustainable solutions.

**Keywords:** photocatalysts; antimicrobial mechanism; reactive oxygen species (ROS); generation; diffusion

## 1. Introduction

With the continuous growth of the global population and the acceleration of urbanization, public health issues are becoming increasingly prominent [1–3]. Bacterial infections have always been a major threat to human health [4,5]. According to statistics, infections caused by pathogenic microorganisms such as bacteria, fungi, protozoa, and other microbes result in millions of deaths worldwide each year [6]. The widespread use of antibiotics has alleviated this issue to some extent [7]. Antibiotics work by disrupting the synthesis of proteins during cell growth, inhibiting the production of DNA or RNA, and preventing the formation of cell membranes and cell walls, ultimately leading to cell death [8]. However, the high dosage and improper use of antibiotics have gradually increased bacteria's resistance to common antibiotics [9], giving rise to superbugs such as methicillin-resistant *Staphylococcus aureus* (MRSA), multidrug-resistant *Staphylococcus pseudintermedius* (MDRSP), and vancomycin-resistant enterococcus (VRE). This phenomenon not only limits the choice of antibiotics but also increases the difficulty and cost of treatment, posing a significant challenge to global public health security. Therefore, finding new antimicrobial methods has become an urgent issue.

Due to its unique advantages and potential, photocatalysis has attracted widespread attention as an emerging antimicrobial technique. The working principle of photocatalytic disinfection is mainly based on its unique electronic structure and band structure. By absorbing light of an appropriate wavelength, electrons from a photocatalyst are excited into a conduction band, and electron-hole pairs are generated. These electron-hole pairs possess strong redox capabilities, capable of decomposing water and organic substances to generate highly



oxidative hydroxyl radicals, superoxide radicals, and singlet oxygen, among other reactive species [10]. These reactive species exhibit high reactivity and can damage the cell walls and membranes of bacteria, disrupt DNA, inactivate enzymes, and achieve bacteriostatic and bactericidal effects. Compared to traditional antibiotics, photocatalysis offers advantages such as high efficiency [11], broad spectrum [12], and environmental friendliness [13], providing a new approach to addressing bacterial resistance issues.

Photocatalytic materials have been extensively researched since the discovery of the photocatalytic water-splitting reaction in 1972 [14]. Based on the composition and structural characteristics of photocatalysts, they can be classified into several categories, including metal oxides [15], MOFs [16], carbon substrates [17], MXenes [18], and more. However, the narrow photoresponse range [19], inappropriate bandgap structure [20], and slow electron circulation [21] greatly restrict the generation of ROS, thus, the diffusion and efficient use of ROS are inhibited, resulting in low antibacterial activity of photocatalysts. ROS are produced by photocatalysts on their surface and typically possess relatively brief half-lives ( $t_{1/2}$ ) and migration distances ( $\lambda$ ). The diffusion distance of  $^1\text{O}_2$  has been reported to be about 0.01–0.02  $\mu\text{m}$ , whereas the thickness of micron-sized bacterial biofilms far exceeds the diffusion distance of  $^1\text{O}_2$  [22]. The  $\bullet\text{OH}$  only impacts bacterial cells within a few nanometers ( $\bullet\text{OH} = 1 \text{ nm}$ ) of where it is generated. Due to its very brief half-life ( $t_{1/2} = 1 \mu\text{s}$ ), it is improbable that  $\bullet\text{OH}$  substances will travel to the cell and harm biomolecules in the majority of instances. The underuse of ROS restricts the overall bactericidal efficacy of photocatalysis. A thorough analysis of various strategies is provided in order to improve the effectiveness of ROS diffusion and utilization, including morphological control, the deposit of noble metals, doping, loading co-catalysts, introducing vacancies, functionalizing surfaces, and creating heterojunctions (Figure 1). Additionally, environmental factors such as pH, temperature, and light intensity [23–25] significantly limit the efficacy of photocatalysis. Therefore, a thorough investigation of the antimicrobial mechanisms of photocatalysts, optimization of the performance and processes of photocatalytic materials, exploration of efficient photocatalytic system designs, and other related aspects are essential.

This review explores the mechanisms of ROS generation and strategies to enhance their diffusion and utilization in photocatalytic materials, focusing on improving their antimicrobial efficacy. It provides a detailed analysis of recent advancements and future prospects in photocatalytic antimicrobial technologies. Moreover, it examines the practical applications of these materials in healthcare, drinking water disinfection, and air purification. By comprehensively analyzing the benefits and challenges associated with photocatalytic technology, we aim to provide robust theoretical support and actionable guidance to further its development. This effort seeks to foster the broad implementation of photocatalytic technology in antimicrobial and disinfection applications, thereby making a significant contribution to the safeguarding of human health and environmental safety.

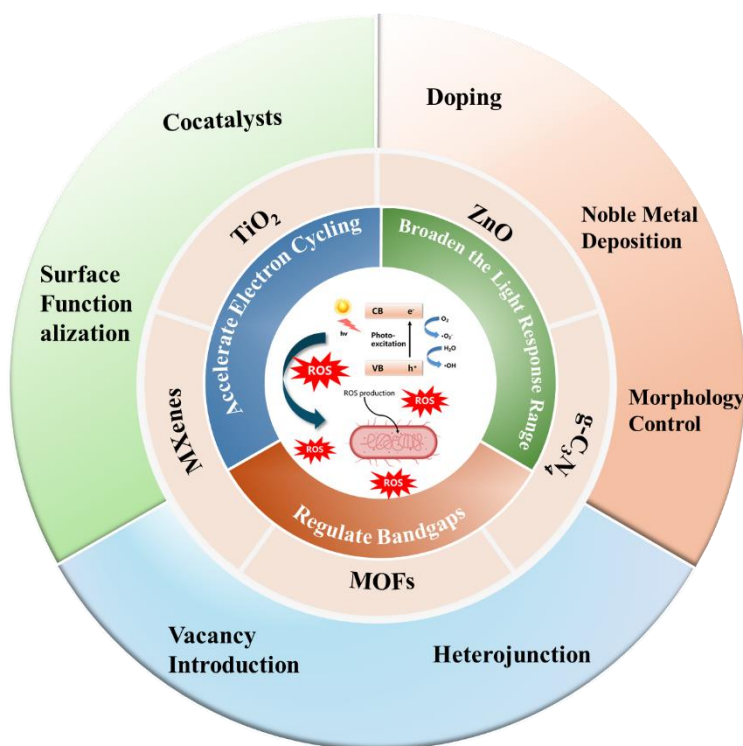


**Figure 1.** Classification of typical photocatalytic antimicrobial agents, principles, and strategies to improve the antimicrobial performance.

## 2. Antibacterial Principle of Photocatalyst

### 2.1. Mechanism of ROS Production in Photocatalytic Reactions

In the 1970s, Fujishima and Honda [14] made the groundbreaking discovery that TiO<sub>2</sub> electrodes can split water into hydrogen under UV light exposure. This finding has since sparked extensive discussions on the application of photocatalysis technology for addressing environmental and energy-related challenges [26]. Photocatalysis typically involves three distinct stages: light excitation, electron and hole migration, and catalytic surface reactions. By absorbing photons with higher energies than the band gap, the photocatalyst creates excited electrons that transition from the valence band to the conduction band, and a pair of electrons and holes is formed by leaving the same number of holes in the valence band (Equation (1)). Positively charged holes and negatively charged electrons migrate to the catalyst surface from the interior. During the migration process, photogenerated carriers may recombine. Light and heat are released, hence decreasing the separation efficiency of electron-hole pairs, and uncombined electrons and holes migrate toward the catalyst surface for redox reactions. Superoxide radicals are formed when electrons e<sup>-</sup> in conduction bands trap molecular oxygen (Equation (2)). Meanwhile, the hole h<sup>+</sup> can react with H<sub>2</sub>O or OH<sup>-</sup> to form a radical called •OH (Equations (3) and (4)). In addition, some •O<sub>2</sub><sup>-</sup> can also react with h<sup>+</sup> to form <sup>1</sup>O<sub>2</sub> (Equation (5)). As highly active oxidants, •OH, •O<sub>2</sub><sup>-</sup> and <sup>1</sup>O<sub>2</sub> can oxidize an indiscriminate range of organic substances.



#### 2.1.1. A Powerful Oxidizing Agent—•OH

In the photocatalytic process, the generation of reactive oxygen species is crucial, among which the •OH is considered one of the most effective oxidizing agents due to its high reactivity and strong oxidative capability. It is generally believed that the oxidation by h<sup>+</sup> in the VB is the primary pathway for •OH generation [27]. Given its high oxidative potential and non-selectivity, •OH can rapidly oxidize most organic compounds, making it particularly important in the study of photocatalytic oxidation reactions. Firstly, the generation of •OH depends on the presence of active sites on the catalyst surface, which can capture H<sub>2</sub>O to produce surface hydroxyl groups, a key intermediate in the formation of •OH. Surface hydroxyl groups are categorized into bridging hydroxyl groups and terminal hydroxyl groups based on their functional group coordination numbers [28]. The protonation of bridging oxygen ions and the pH value of the solution significantly influence the generation rate and yield of these hydroxyl groups. It is important to note that •OH radicals cannot directly penetrate cell membranes; thus, they primarily act on the cell surface, where they react with structural components of the cell membrane or cell wall.

#### 2.1.2. Highly Reactive Radical Intermediate—•O<sub>2</sub><sup>-</sup>

In photocatalytic reactions, the generation of •O<sub>2</sub><sup>-</sup> mainly occurs through two pathways: the single-electron reduction of O<sub>2</sub> and the oxidation of H<sub>2</sub>O<sub>2</sub>. Because O<sub>2</sub> readily accepts electrons and is reduced, the quantum yield of •O<sub>2</sub><sup>-</sup> is very high in the initial stages of photocatalytic reactions. In these reactions, the excited e<sup>-</sup> in the CB reduces O<sub>2</sub> to produce •O<sub>2</sub><sup>-</sup>, which plays a dominant role in the generation of reactive oxygen species. According to semiconductor band theory, the more negative the conduction band position relative to the reduction potential of O<sub>2</sub>/•O<sub>2</sub><sup>-</sup>, the stronger the electron's reducing ability, and the higher the likelihood of •O<sub>2</sub><sup>-</sup> production. However, due to the principle of like-charge repulsion, hydrophilic negatively charged •O<sub>2</sub><sup>-</sup> has difficulty penetrating the negatively charged cell membrane composed of phosphate groups. Consequently, •O<sub>2</sub><sup>-</sup> attacks bacterial cell membranes, leading to the leakage of cellular contents and causing irreversible cell damage [29]. By understanding the relationship between the reducing ability of conduction band electrons and •O<sub>2</sub><sup>-</sup> production, it is possible to further optimize photocatalytic materials to enhance their effectiveness in antibacterial applications.

### 2.1.3. The Excited State of Molecular Oxygen— $^1\text{O}_2$

$^1\text{O}_2$ , a highly reactive and oxidative form of oxygen, is gaining attention for its potential applications in selective organic synthesis, pollutant degradation, and bacterial inactivation. The excited state of the dioxygen molecule,  $^1\text{O}_2$ , exhibits significantly higher reactivity compared to its ground state. The generation of  $^1\text{O}_2$  on the surface of photocatalytic materials involves three key steps: adsorption of triplet molecular oxygen, single-electron reduction, and electron-loss oxidation [30]. The generation of  $^1\text{O}_2$  is initiated by the adsorption of triplet molecular oxygen onto the photocatalyst surface, followed by single-electron reduction (Equation (2)) and subsequent oxidation (Equation (5)). The resulting  $^1\text{O}_2$ , characterized by its high reactivity, is quenched on the catalyst surface and dissociatively reduced to molecular oxygen. The process that determines the rate of this is the redox capacity of the photogenerated charge carriers. Intersystem crossing (ISC) allows long-lived triplet excitons to develop in conjugated polymers by transferring the singlet excited state to the low-energy triplet excited state [31]. The efficiency of ISC is crucial, as higher ISC efficiency results in a greater concentration of triplet excitons. However, the efficiency of  $^1\text{O}_2$  creation via triplet excitons is naturally limited in many conjugated polymers, as only a small fraction of singlet excitons can transition to triplet excitons before being quenched. To enhance the generation of  $^1\text{O}_2$ , it is essential to optimize the exciton processes in conjugated polymers. To develop oxidized g- $\text{C}_3\text{N}_4$  (CNO) and increase the yield of triplet excitons, Wang et al. introduced carbonyl groups into the g- $\text{C}_3\text{N}_4$  polymer matrix using a straightforward oxidation technique [32]. ESR measurements of CNO and the original g- $\text{C}_3\text{N}_4$  revealed a substantial increase in the efficiency of  $^1\text{O}_2$  generation, while the production of other ROS was suppressed. The study found that the removal of carbonyl groups greatly reduced the generation of  $^1\text{O}_2$ , indicating that the carbonyl groups on CNO are responsible for the production of  $^1\text{O}_2$ .

### 2.1.4. Reactive Oxygen Species with Persistent Bactericidal Activity— $\text{H}_2\text{O}_2$

$\text{H}_2\text{O}_2$  is widely recognized for its stable thermodynamic state, long lifespan, and consistent oxidative capabilities. These properties make  $\text{H}_2\text{O}_2$  a crucial element in ensuring the prolonged bactericidal activity of photocatalytic antibacterial materials. The generation of  $\text{H}_2\text{O}_2$  occurs through two main pathways: the  $2e^-$  reduction of  $\text{O}_2$  and the  $2h^+$  oxidation of  $\text{H}_2\text{O}$  [33]. Among these, the reduction pathway is predominant due to the low reactivity of  $\bullet\text{O}_2^-$ . As a small and diffusible molecule,  $\text{H}_2\text{O}_2$  can penetrate bacterial cell membranes, reaching intracellular targets where it reacts with various proteins and enzymes. This interaction disrupts the cell's selective permeability, leading to an imbalance of substances inside and outside the cell, ultimately causing bacterial death. Furthermore, intracellular  $\text{H}_2\text{O}_2$  can be enzymatically decomposed to form  $\bullet\text{OH}$ , which is highly reactive and capable of initiating a series of oxidative chain reactions. These reactions attack membrane structures, increase lipid peroxidation damage, and allow more free radicals to penetrate the cell, thereby enhancing the degree of bacterial cell damage. Despite its potent bactericidal effects, the efficiency of  $\text{H}_2\text{O}_2$  as an antibacterial agent is compromised under certain conditions. Exposure to light or heat catalyzes the decomposition of  $\text{H}_2\text{O}_2$  into  $\bullet\text{OH}$ , which, while highly reactive, reduces the overall antibacterial efficiency of  $\text{H}_2\text{O}_2$ .

## 2.2. General Process and Influencing Factors of ROS Diffusion

The diffusion of ROS generated by photocatalytic reactions is a complex process influenced by multiple factors [34]. Understanding the mechanisms of ROS diffusion is crucial for optimizing the antimicrobial efficacy of photocatalytic materials. ROS such as  $\bullet\text{OH}$ ,  $\bullet\text{O}_2^-$ ,  $\text{H}_2\text{O}_2$ , and  $^1\text{O}_2$  are generated on the surface of photocatalysts upon light irradiation. The initial generation involves the excitation of electrons to the conduction band, creating electron-hole pairs. These electron-hole pairs participate in redox reactions that produce ROS. For instance, water oxidation typically generates  $\bullet\text{OH}$ , while oxygen reduction can lead to the formation of  $\bullet\text{O}_2^-$  and subsequently  $\text{H}_2\text{O}_2$ . Once generated, ROS must diffuse away from the photocatalyst surface to interact with microbial cells. This diffusion is influenced by the medium in which the photocatalyst is suspended. In aqueous systems, the mobility and reactivity of ROS can be significantly different compared to gaseous environments [35].

Several factors influence the diffusion process. The surface area, porosity, and the presence of surface defects or functional groups of the photocatalyst play a critical role in its physical and chemical properties. High surface area and porosity facilitate the migration of ROS from the generation site to the bulk medium. Additionally, the viscosity and composition of the medium affect ROS mobility; lower viscosity in aqueous solutions promotes faster diffusion, while organic and inorganic substances in the medium can impact ROS stability and availability for antimicrobial action. Organic matter, for instance, can act as scavengers, reducing ROS effectiveness. Temperature and pH levels also significantly affect ROS diffusion and stability. Higher temperatures generally enhance diffusion rates by increasing kinetic energy, though they may also accelerate ROS recombination. The pH level affects ROS stability differently;  $\bullet\text{OH}$  is more stable in neutral to slightly acidic conditions, while  $\bullet\text{O}_2^-$  is

stabilized in alkaline environments. Environmental conditions, such as humidity and light, further influence ROS diffusion efficiency. High humidity levels enhance ROS mobility and prolong their lifetime, while light intensity and wavelength determine ROS generation rates and subsequent diffusion. The inherent stability of different ROS types is another critical factor. Some highly reactive ROS, such as hydroxyl radicals, have a short lifetime in solution due to their propensity to react with other substances [36]. On the other hand, H<sub>2</sub>O<sub>2</sub> has a stable thermodynamic state and a longer lifetime in solution due to its ability to oxidize other compounds [29]. For ROS to exert their antibacterial effect, their diffusion distance must be sufficient to reach bacterial cell walls or membranes, leading to oxidative reactions that destroy cell structures and result in cell death. However, the short diffusion distance of ROS often results in a low utilization rate. The development of a nano-confined catalytic system can enhance mass transfer kinetics and optimize its utilization rate. Furthermore, Li et al. discovered that incorporating a hydrophobic microenvironment can impede the diffusion of the hydrophilic interface of the reactants, effectively confining ROS from oxidizing pollutants in the hydrophilic region, thus significantly enhancing their utilization rate [37].

### 2.3. ROS for Photocatalytic Antibacterial Activity

Photocatalysis has emerged as a potential technique in the realm of antimicrobial technology because of its capacity to generate ROS, which can efficiently inhibit and eradicate a variety of infections. Photocatalysis, which utilizes light energy to drive chemical reactions, has received much research attention due to its potential for disinfecting and cleaning environments. The generation of reactive oxygen species, such as hydroxyl radicals, hydrogen peroxide, and superoxide anion [38], plays a crucial role in the antimicrobial action of photocatalysis. These oxidizing and damaging compounds cause lipids, proteins, and DNA in microbial cells to break down and eventually die. The effectiveness of ROS generation and antibacterial action depends on the choice of photocatalytic materials. Because of its superior photocatalytic efficiency and chemical stability, TiO<sub>2</sub> has drawn much attention from researchers. When TiO<sub>2</sub> is exposed to photoexcitation, it can generate ROS, which possess potent oxidative characteristics that can efficiently damage bacterial cell walls and membranes, hence impeding their growth and reproduction. Its broad bandgap, however, restricts its action to ultraviolet light, which makes up only 5% of the solar spectrum. Several approaches, such as doping with metals or non-metals, interfacing with other semiconductors to generate heterojunctions, and generating oxygen vacancies, have been investigated by researchers to circumvent this restriction.

To enhance the production efficiency of ROS, Yan et al. [39] created a binary composite direct Z-scheme heterostructure CeO<sub>2</sub>/TiO<sub>2</sub> NTAs. This NTA exhibits good antimicrobial effects against both Gram-positive and Gram-negative bacteria, maintaining a disinfection efficiency of 98.3% after three cycles of disinfection experiments. Under illumination, it achieves spatial separation of oxidation and reduction sites, facilitating the production of ROS. Wang et al. [40] reported that the inactivation of *E. coli* was found to be greatly accelerated by the photocatalytic process in the UV+NF@TiO<sub>2</sub> system. According to the EPR data, photocatalytically generated •O<sub>2</sub><sup>-</sup> and •OH were the primary causes of *E. coli* inactivation. However, *E. coli* leaks biomolecules that block the pores of NF@TiO<sub>2</sub>, reducing its bactericidal performance and causing photocatalyst poisoning after 70 cycles (Figure 2). Therefore, it is essential to develop photocatalysts with high antibacterial activity to prevent pore blockage. Despite significant progress, several challenges remain to be addressed. Rapid electron-hole pair recombination is a significant problem that lowers ROS generation efficiency overall and restricts the use of photocatalysis in the antibacterial field. To overcome this challenge, several innovative studies have been conducted. To increase the generation of electron-hole pairs, some research focuses on creating novel semiconductor materials that can absorb a wider range of visible light. Additionally, the recombination of electron-hole pairs can be successfully reduced by adding particular dopants or coatings to the photocatalyst's surface, increasing the efficiency of ROS formation. Furthermore, some studies have explored the regulation of electron-hole pair behavior through external electric or magnetic fields to improve their separation efficiency. Another key aspect is the potential toxicity of photocatalytic materials and the ROS they produce to human cells and the environment. Studies have shown that while ROS kill bacteria, they can also cause oxidative stress in mammalian cells. Therefore, understanding the cytotoxicity of photocatalytic materials and their environmental impact is crucial for safe application.

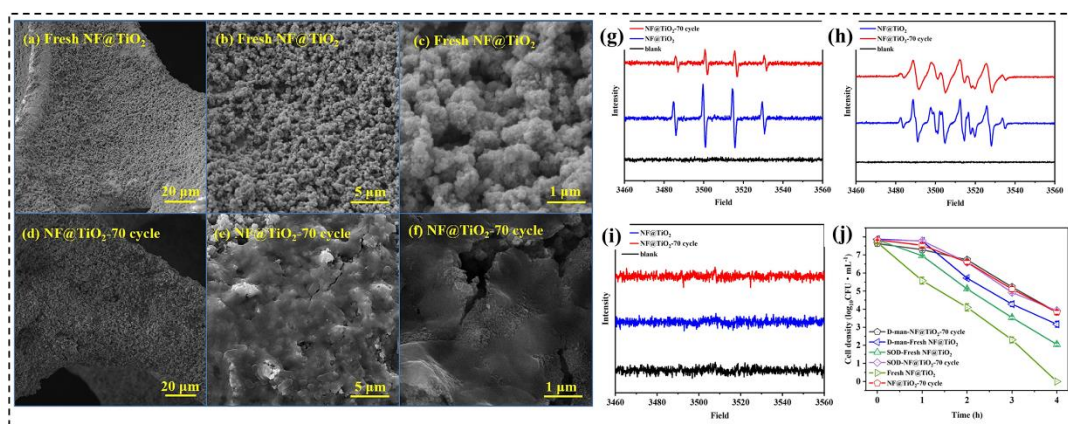


**Figure 2.** (a–f) Repeated photocatalytic inactivation of *E. coli* by UV + Ni foam@TiO<sub>2</sub>: Performance and photocatalyst deactivation. EPR spectra of (g) DMPO-•OH, (h) DMPO-•O<sub>2</sub><sup>-</sup>, (i) TEMP-<sup>1</sup>O<sub>2</sub> in UV + fresh TiO<sub>2</sub> and UV + used TiO<sub>2</sub> systems, and (j) the influence of various radical scavengers on the inactivation of *E. coli*. Ref. [40] reproduced with permission. Copyright 2023, Elsevier.

### 3. Progress on Photocatalytic Antimicrobial Materials

#### 3.1. TiO<sub>2</sub>

Metal oxide photocatalysts, particularly TiO<sub>2</sub> [41], ZnO [42], and SiO<sub>2</sub> [43], these materials have been thoroughly researched for their capacity to utilize light energy in diverse applications such as environmental cleanup, energy transformation, and antimicrobial uses. The semiconducting properties of these substances are mainly responsible for their photocatalytic performance, as they facilitate the creation of electron-hole pairs through light absorption. TiO<sub>2</sub> has garnered significant attention as a photocatalyst for its remarkable ability to efficiently drive photoreactions, maintain chemical robustness, and demonstrate a non-hazardous nature [44]. Within the realm of TiO<sub>2</sub> photocatalysis, electrons are energetically elevated from the valence band (VB) to the conduction band (CB) through light absorption, with a particular focus on the ultraviolet (UV) spectrum. Electrons and holes generated can travel to the surface, engaging in redox reactions that trigger the creation of ROS, like •OH, •O<sub>2</sub><sup>-</sup>, and H<sub>2</sub>O<sub>2</sub>. These substances facilitate the breakdown of organic pollutants and rendering microorganisms inactive. Doping with elements such as nitrogen, carbon, or iron can reduce the TiO<sub>2</sub> bandgap, create mid-gap states, and enhance light absorption and ROS generation under visible light. Huang et al. [45] prepared an N-doped TiO<sub>2</sub> with sufficient OV<sub>s</sub> under NH<sub>3</sub> atmosphere. Incorporating nitrogen into TiO<sub>2</sub> can result in the generation of Ti-O-N/O-Ti-N-O. This incorporation leads to the creation of oxygen vacancies, which play a crucial role in enabling the absorption of oxygen molecules on the surface of TiO<sub>2</sub>, giving rise to •O<sub>2</sub><sup>-</sup>. Consequently, this mechanism enhances the efficiency of separating and transporting electrons and holes produced through illumination. The band gap of TiO<sub>2</sub> can be determined using the  $(\alpha\text{-}h\nu)^2\text{-}h\nu$  relationship. The bandgaps of TiO<sub>2</sub>, 1-N-TiO<sub>2</sub>, and 4-N-TiO<sub>2</sub> are 3.35 eV, 3.33 eV, and 3.26 eV, respectively (Figure 3a,b). Spectrophotocurrent spectroscopy studies examine the ability of photo-excited carriers to separate in these materials. N-doped TiO<sub>2</sub> photocatalysts exhibit more pronounced response peaks in the UV range compared to regular TiO<sub>2</sub>. Furthermore, the newly observed SPS response in the 380–450 nm region demonstrates the visible light capabilities and photocatalytic properties of N-TiO<sub>2</sub>. Additionally, surface treatment with noble metals or metal oxides can increase photocatalytic performance and electron-hole pair separation. The inability of metal single atoms (SAs) to control the band gap of the carrier photocatalyst is due to their propensity to aggregate during synthesis and reaction. To fully expose metal SAs and adjust the band gap of photocatalysts, Xiao et al. [46] proposed a surface doping approach to increase the photocatalytic activity of TiO<sub>2</sub> by combining the benefits of high SA activity with doping energy band control. Under 365 nm light irradiation, the ideal CuSAs-TiO<sub>2</sub> has an apparent quantum efficiency of 6.03% (Figure 3c,d). The rapid synthesis of pure TiO<sub>2</sub> semiconductor photoelectron-hole pairs limits the photocatalytic efficiency to a large extent. Constructing heterogeneous composite materials from two or more kinds of semiconductors can induce spatial separation of charge carriers, achieve efficient electron transfer, and improve the efficiency of ROS generation. Using a hydrothermal process, Chen et al. [47] created a TiO<sub>2</sub>/TiOF<sub>2</sub> heterojunction catalyst with a well-matched interface. At a low concentration of 110 μg/mL, the TiO<sub>2</sub>/TiOF<sub>2</sub> material demonstrated 81.89% antibacterial efficiency against *S. aureus* and 99.90% antibacterial efficiency against *E. coli* (Figure 3e,f). In addition to facilitating photogenerated electron migration from TiO<sub>2</sub> to TiOF<sub>2</sub> and their subsequent capture by adjacent H<sub>2</sub>O and O<sub>2</sub> molecules to form corresponding surface reactive oxygen species

•O<sub>2</sub><sup>-</sup> and •OH, the heterojunction between TiO<sub>2</sub> and TiOF<sub>2</sub> may efficiently regulate the band structure. Physical harm and the release of F also play a supporting role in the antibacterial process.

Given its excellent photocatalytic efficacy, chemical stability, and lack of toxicity, TiO<sub>2</sub> is one of the most commonly utilized photocatalysts. It effectively generates •OH and •O<sub>2</sub><sup>-</sup> under UV light, leading to the destruction of bacterial cell walls and DNA. TiO<sub>2</sub> is extensively used in coatings for medical devices and air purifiers, where its ability to inactivate bacteria such as *S. aureus* and *Escherichia coli* (*E. coli*) has been well-documented. Comparatively, TiO<sub>2</sub> tends to be more effective against Gram-positive bacteria, such as *S. aureus*, due to the simpler structure of their cell walls compared to the more complex outer membrane of Gram-negative bacteria like *E. coli*. However, under optimized photocatalytic conditions or through doping, TiO<sub>2</sub> can effectively target Gram-negative species as well. Nevertheless, there are notable limitations to the use of TiO<sub>2</sub> in antibacterial applications. A primary limitation is its reliance on UV light to activate its photocatalytic properties, which restricts its effectiveness in indoor environments where UV light exposure is limited. Additionally, although TiO<sub>2</sub> is generally considered safe, concerns about its cytotoxic effects at high concentrations or with prolonged exposure necessitate careful consideration, especially in medical applications. Another challenge is the tendency of TiO<sub>2</sub> nanoparticles to agglomerate, which reduces their surface area and antibacterial efficacy.

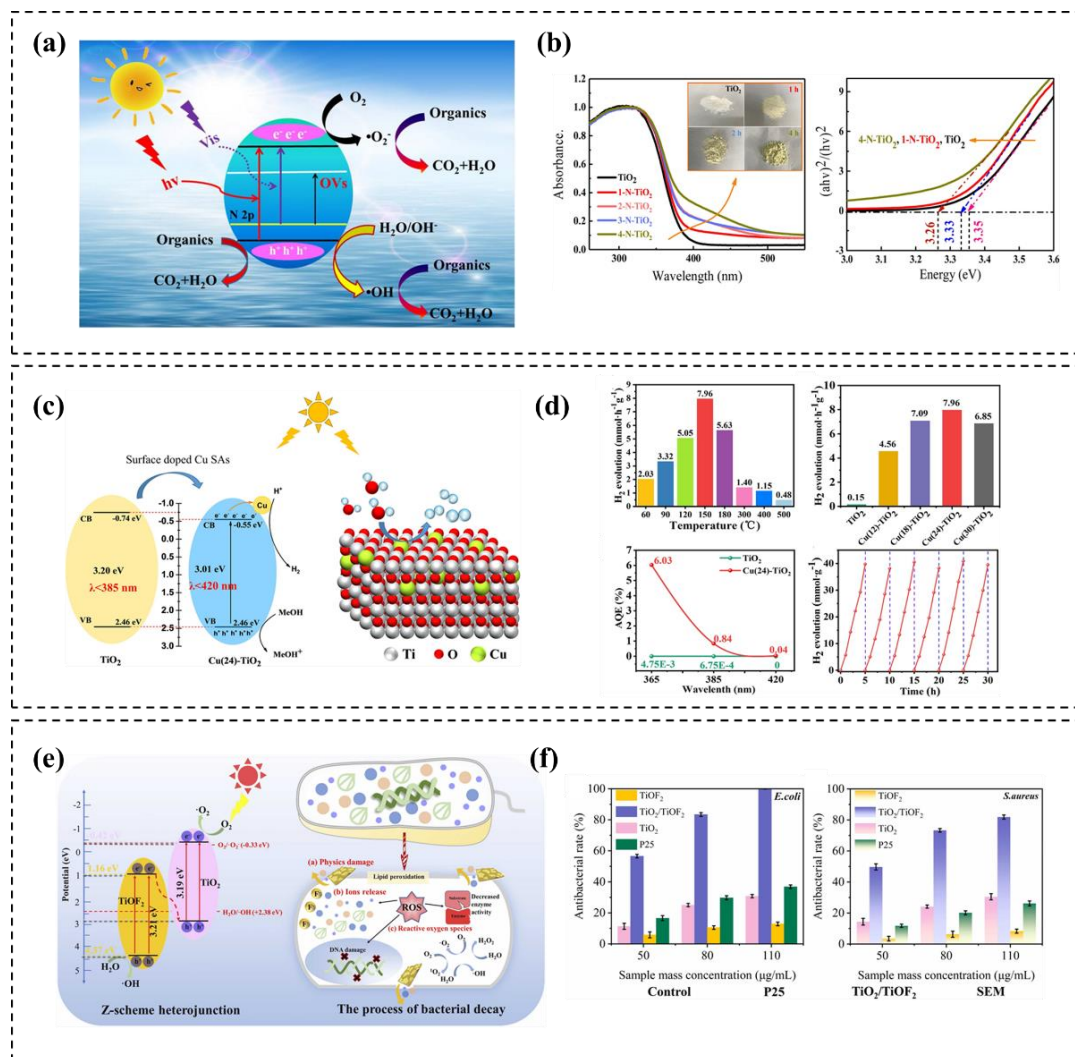


**Figure 3.** (a) Photocatalytic mechanism of N-doped TiO<sub>2</sub> photocatalysts. (b) UV-vis diffuse reflectance spectra and band gaps of the catalysts; Ref. [45] reproduced with permission. Copyright 2021, Elsevier. (c) Photocatalytic hydrogen production mechanism of CuSAs-TiO<sub>2</sub> constructed by Cu surface doping (d) Average HER of CuSAs-TiO<sub>2</sub> with the same addition of 24 mg CuCl<sub>2</sub> and different heat treatment temperature under the irradiation of 300 W Xe-lamp; average HER under the irradiation of 300 W Xe-lamp at the same heat treatment temperature (150 °C) and different Cu content; AQE of TiO<sub>2</sub> and Cu(24)-TiO<sub>2</sub> under the irradiation of LED lamp with wavelength 365 nm, 385 nm, 420 nm, respectively; cyclic stability test of Cu(24)-TiO<sub>2</sub> irradiated by 300 W Xe-lamp. Ref. [46] reproduced with permission. Copyright 2023, Elsevier. (e) Schematic illustration of the Z-scheme heterojunction and the process of bacterial decay

antibacterial mechanisms of TiO<sub>2</sub>/TiOF<sub>2</sub> nanosheets. (f) The antibacterial effect with TiO<sub>2</sub>/TiOF<sub>2</sub> and P25 under white light for 30 min on *E. coli* and *S. aureus*. Ref. [47] reproduced with permission. Copyright 2024, Elsevier.

### 3.2. ZnO

Because of its strong oxidizing abilities and narrow bandgap, ZnO has become a viable photocatalyst. Similar to TiO<sub>2</sub>, ZnO produces ROS when exposed to light, which has the ability to efficiently break down contaminants and eradicate microorganisms. Regulating its shape and structure enhances the ZnO's photocatalytic efficacy. ZnO nanowires, nanoparticles, and nanosheets have been synthesized and shown to exhibit enhanced photocatalytic activity compared to bulk ZnO. Nanostructured photocatalysts offer a larger surface area for ROS generation and diffusion. This increased surface area enhances the contact between ROS and microbial cells, thereby improving antimicrobial efficacy. Additionally, the formation of ZnO-based composites with other materials, such as ZnO/TiO<sub>2</sub> or ZnO/Ag, has been demonstrated to enhance the separation of electron-hole pairs and improve photocatalytic efficiency. However, the exact antibacterial mechanism of ZnO NPs under visible light irradiation remains unclear. To study how *S. aureus* is inactivated by amino-functionalized hydrophilic ZnO (AH-ZnO) NPs in aqueous environments when exposed to visible light, Du et al. prepared amino-functionalized AH-ZnO NPs modified with 3-aminopropyltriethoxysilane [48] (Figure 4). The outcomes showed that the antibacterial activity of AH-ZnO NPs is contingent upon both the concentration and duration of treatment. With an increase in AH-ZnO NPs concentration, there was a corresponding increase in the volume Oxidation-reduction potential (ORP) value and the concentration of liberated Zn<sup>2+</sup> in the AH-ZnO NPs solution. The antibacterial mechanism of AH-ZnO NPs involves multiple synergistic effects. Under visible light irradiation, AH-ZnO NPs are excited, causing electrons to transition from the VB to the CB, producing several photogenerated electrons and holes on their surface. The CB of AH-ZnO NPs transfers these free electrons to the respiratory chain proteins on the *S. aureus* cell membrane. A rise in ORP results from the highly reactive holes' reaction with water to produce •OH. The PL intensity and fluorescence lifespan of AH-ZnO NPs are decreased by the interfacial electron transfer, which also prevents photogenerated electron-hole pairs from recombining. The transferred electrons disrupt the normal electron transport process, causing a large number of electrons to leak from the respiratory chain proteins into the cytoplasm, where they react with oxygen to form •O<sub>2</sub><sup>-</sup>. These radicals are then converted to H<sub>2</sub>O<sub>2</sub> by Superoxide Dismutase (SOD) and subsequently generate more •OH through the Fenton reaction, leading to excessive intracellular ROS generation. In the meantime, the compromised respiratory chain depolarizes the bacterial cell membrane by preventing protons from being pumped from the inside to the outside. There is a drop in intracellular ATP levels because the lowered proton electrochemical gradient cannot supply enough proton motive force required for the ATP synthase function. Ultimately, *S. aureus* undergoes an apoptosis-like process that results in the generation of intracellular ROS and the breakdown of ATP synthesis.

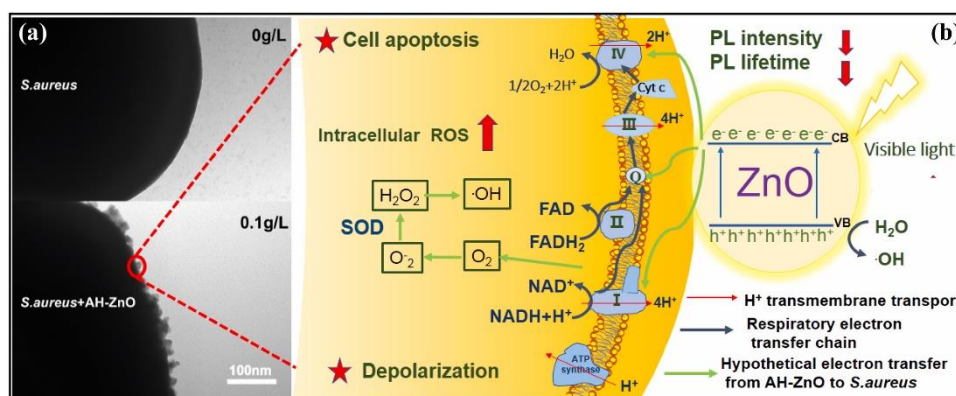


**Figure 4.** (a) TEM image of *S. aureus* and *S. aureus*/AH-ZnO NPs composites. (b) Schematic diagram of the visible-light-driven photocatalytic inactivation of *S. aureus* by AH-ZnO NPs based on the interfacial electron transfer in *S. aureus*/ZnO composites. Ref. [48] reproduced with permission. Copyright 2021, Elsevier.

ZnO exhibits strong antibacterial activity against a broad spectrum of bacteria due to its ability to produce ROS and release Zn<sup>2+</sup> ions, which contribute to its antimicrobial properties. ZnO has been particularly effective in targeting *S. aureus* and *Pseudomonas aeruginosa*. The ROS production by ZnO nanoparticles is not only effective under light but also in dark conditions due to the presence of surface defects that facilitate ROS generation even without photoactivation. When exposed to UV light, the antibacterial activity of ZnO nanoparticles is further enhanced due to increased ROS production, which is advantageous in applications requiring rapid sterilization and



disinfection. Additionally, the effectiveness of ZnO nanoparticles is size-dependent; smaller particles offer a larger surface area for bacterial interaction, leading to enhanced antibacterial effects. However, the use of ZnO nanoparticles is not without challenges. One major concern is cytotoxicity, as the ROS generated can also harm human cells, potentially limiting biomedical applications. Furthermore, ZnO nanoparticles can release zinc ions, which contribute to antibacterial activity but also pose environmental and health risks due to potential toxicity.

### 3.3. $g\text{-C}_3\text{N}_4$

Since  $g\text{-C}_3\text{N}_4$  was first reported as a metal-free semiconductor photocatalyst for  $\text{H}_2$  reduction, it has been widely applied in water splitting,  $\text{CO}_2$  reduction, photocatalytic degradation of organic compounds, and other fields. Composed of a two-dimensional layered structure,  $g\text{-C}_3\text{N}_4$  is similar to graphene. Through  $\text{sp}^2$  hybridization, carbon and nitrogen atoms produce a  $\pi\text{-}\pi$  conjugated electronic structure, which subsequently stacks repeatedly to form a three-dimensional crystalline structure. The pure  $g\text{-C}_3\text{N}_4$ , however, has limited visible light utilization due to numerous defects, significantly restricting its widespread application. The inherent rapid electron-hole recombination within the photocatalyst and the short migration distance of bacteria cells and photogenerated ROS at the biointerface result in reduced antibacterial activity. In order to optimize the ROS reaction during photocatalysis and reduce the distance between ROS and bacterial cells, Zhu et al. designed a hybrid photocatalyst,  $g\text{-C}_3\text{N}_4/\text{MIL-125-NH}_2$ , a hybrid photocatalyst that has a positively charged quaternary ammonium compound (QAC) polymer surface layer that increases its electrostatic attraction to bacterial cells [49] (Figure 5). This surface-modified photocatalyst is labeled as  $\text{QAC}@g\text{-C}_3\text{N}_4/\text{MIL-125-NH}_2$ . Through electrostatic attraction, the positively charged QAC layer facilitates contact between the bacteria and the photocatalyst. The synergistic effect of bacterial cell adhesion and ROS generation significantly enhances the photocatalyst's POD performance. The force-distance relationship between  $\text{QAC}@g\text{-C}_3\text{N}_4/\text{MIL-125-NH}_2$  and bacterial cells was measured using atomic force microscopy (AFM). The results indicate that the MOF-based catalyst's positive charge modulation facilitates bacterial adhesion to the photocatalyst surface. Specifically, a significant adhesion force of 972 pN was observed between the modified cantilever tip and the bacteria, while only 115 pN was detected between the unmodified reference tip and the bacteria. Remarkably, under visible light irradiation, the photocatalyst achieved an inactivation efficiency of 3.20 logs for *Staphylococcus epidermidis* within 60 min. By using electrostatic attraction, this study offers a novel method for enhancing the antibacterial efficacy of photocatalysts by improving the affinity between bacterial cells and the catalyst at the biointerface.

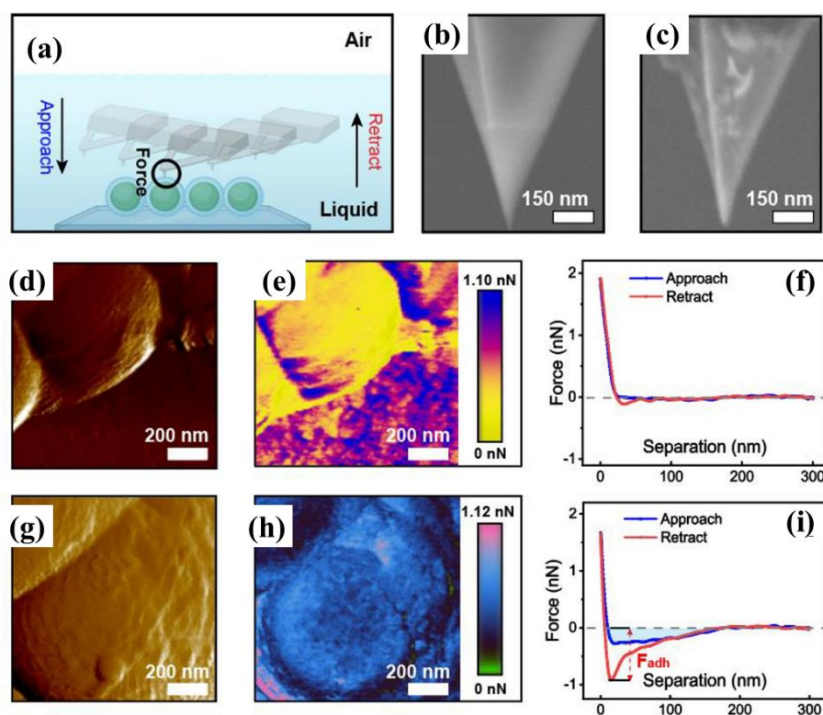


**Figure 5.** AFM force measurements between *S. epidermidis* cells and the photocatalyst. (a) Illustration of the AFM force measurement in PBS solution; SEM images of (b) the pristine AFM Si probe and (c) the  $\text{QAC}@g\text{-C}_3\text{N}_4/\text{MIL-125-NH}_2$  coated Si probe; (d–i) are the peak force error image, adhesion force mapping, and approach-retract force curves of *S. epidermidis* cells measured by using the pristine AFM probe and the photocatalyst-coated probe, respectively. Ref. [49] reproduced with permission. Copyright 2023, Elsevier.

g-C<sub>3</sub>N<sub>4</sub> serves as a metal-free photocatalyst that can be triggered by visible light, rendering it a sustainable and environmentally friendly choice. In antibacterial applications, g-C<sub>3</sub>N<sub>4</sub> offers several distinct advantages. Firstly, it can efficiently generate ROS upon exposure to light, enabling broad-spectrum antibacterial activity against various bacteria, including both Gram-positive and Gram-negative strains, such as *S. aureus* and *E. coli*. Moreover, the excellent chemical stability of g-C<sub>3</sub>N<sub>4</sub> allows it to maintain its activity over extended periods without significant degradation under various environmental conditions. As a metal-free catalyst, g-C<sub>3</sub>N<sub>4</sub> is more environmentally friendly compared to metal-based antibacterial agents, thereby minimizing environmental impact. In addition, g-C<sub>3</sub>N<sub>4</sub> is inexpensive to produce and easy to synthesize from abundant precursor substances such as melamine and urea. This economy makes it ideal for cost-sensitive applications. Finally, the versatility of g-C<sub>3</sub>N<sub>4</sub> is also reflected in the fact that it can be used in diverse forms such as powders, films or composites for different application scenarios such as surface coatings or water treatment systems. Nevertheless, its photocatalytic efficiency is constrained by its narrow bandgap, leading to limited light absorption in low-light conditions. Additionally, the rapid recombination of photogenerated electron-hole pairs limit its photocatalytic efficiency, necessitating modifications such as doping or combining with other materials to enhance performance. Although g-C<sub>3</sub>N<sub>4</sub> is generally considered safe, the ROS generated can pose potential toxicity risks to non-target organisms, which must be considered in certain environmental contexts.

### 3.4. Metal-Organic Frameworks (MOFs)

Metal-organic framework (MOF) materials exhibit a substantial surface area, meticulously arranged porous structure, and customizable organic bridging linker/metal clusters that can efficiently absorb light. This unique combination of features positions them as a highly effective photocatalyst for antibacterial. Recent advancements in the synthesis of MOFs have focused on enhancing their photocatalytic efficacy and stability. For instance, methods such as controlled solvothermal reactions allow for the fine-tuning of MOF structures to optimize their light absorption and reactivity [50]. Researchers have explored the incorporation of various metals like Cu<sup>2+</sup> and Zn<sup>2+</sup> [51] and functional groups into MOF frameworks to tailor their electronic properties and increase their reactive surface area. This customization facilitates the generation of ROS under light irradiation, which is crucial for antibacterial activity. One of the significant challenges with MOFs in photocatalytic applications is their stability under operational conditions. Emphasizing the incorporation of highly reactive metals into MOFs as a savvy strategy to boost the number of active sites is noted to enhance both the photocatalytic performance and longevity of the material. Depositing metal co-catalysts onto the surface of MOFs can effectively enhance the generation and diffusion of ROS. These metals serve as electron sinks, thereby reducing recombination rates and increasing the availability of ROS. Integrating MOFs with nanoparticles such as gold or silver has been shown to induce plasmonic effects, extending the light absorption to the visible range and enhancing the photocatalytic degradation of pollutants and microbes under ambient light conditions. By strengthening charge separation and extending the lifetime of ROS, non-metal co-catalysts can also promote ROS diffusion. Doping MOFs with non-metal elements like carbon or nitrogen have been found to significantly affect their electronic structures, facilitating better charge separation and extending their light absorption capabilities [52]. MOFs have been utilized as photocatalytic materials for the rapid eradication of bacteria and efficient diffusion of ROS in porous environments. Nevertheless, the restricted diffusion distance of ROS still limits the bactericidal effectiveness of MOFs. Close contact between MOFs and bacterial cells can effectively and quickly transmit ROS, which is essential for the photoinactivation of bacteria. Chen et al. creatively introduced boric acid ligands and photosensitive porphyrin Cu(II) into a single Zr-based MOF through a convenient one-pot hydrothermal synthesis strategy, enhancing its antibacterial ability with a synergistic bacteria-binding effect [53] (Figure 6). By covalently attaching to the cis-diol structure found in the carbohydrates on bacterial surfaces, the modification of MOFs with boric acid allows for bacterial identification. Charge transfer and the production of reactive oxygen species are facilitated by copper in the porphyrin ring, which absorbs photoexcited electrons and acts as an active site for proton reduction. The boric acid-modified MOF adheres to bacteria via covalent bonds with abundant surface carbohydrates. The photosensitive porphyrin Cu(II) within the MOF exhibits excellent PDT effects, rapidly inactivating bacteria under light irradiation and generating large amounts of ROS. With the help of Cu(II) and boric acid, which close physical gaps with bacteria and produce more ROS, the highly biocompatible multi-component MOF functions as a regulated broad-spectrum bactericide, rapidly killing bacteria. The multi-component MOF exhibits dramatically improved antibacterial efficacy as compared to MOFs lacking boric acid ligands. Moreover, in vivo tests show that the multi-component MOF can successfully treat long-term wounds affected by MDR Gram-positive or Gram-negative bacteria.

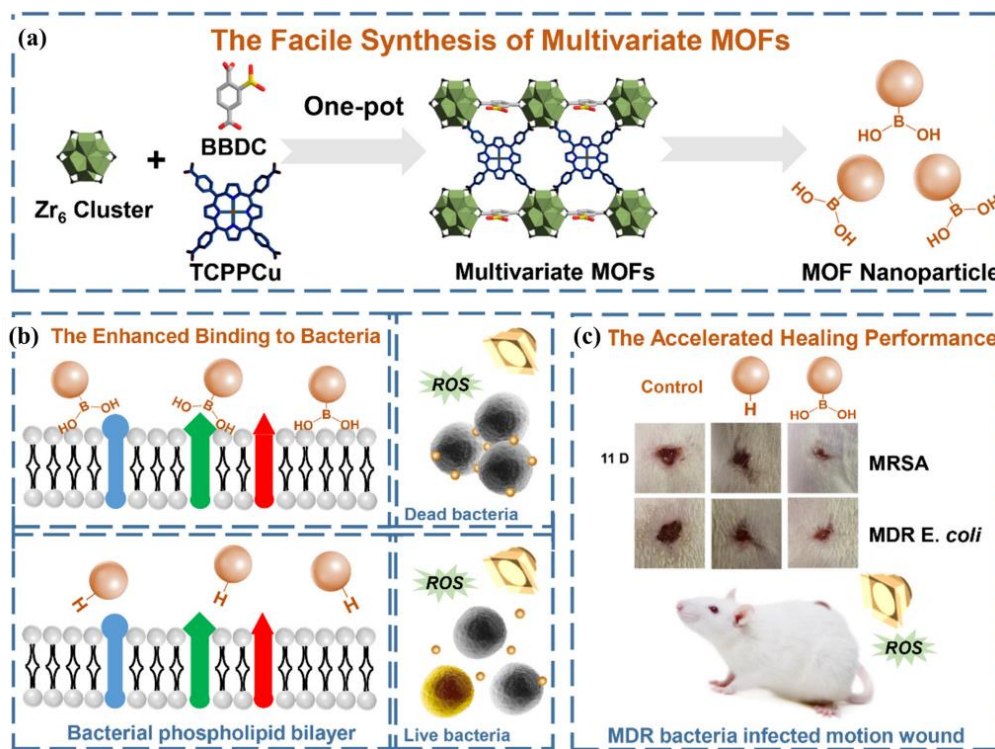


**Figure 6.** Schematic illustration of (a) the facile synthesis of multivariate photosensitive MOFs with synergistic bacterial-binding functions, (b) the bindings of multivariate MOFs to bacteria, and (c), the application for efficient healing of a chronic wound infected with MDR bacteria. Ref. [53] reproduced with permission. Copyright 2022, American Chemical Society.

MOFs boast expansive surface areas and customizable porosity, rendering them exceptionally proficient in trapping and breaking down organic contaminants and pathogens. MOFs exhibit multiple antibacterial mechanisms, including the slow release of metal ions, direct contact with bacteria, the release of small molecule drugs, the ROS under light, enzyme mimicry, and gas therapy, effectively killing bacteria. These mechanisms enable MOFs to target and release antibacterial components in a controlled manner, reducing toxicity and making them suitable for biomedical applications. Ag-MOFs and Zn-MOFs disrupt ion channels and penetrate bacterial membranes, while Cu-MOFs release Cu<sup>2+</sup> to destroy bacterial membranes and DNA. MOFs are effective against a broad spectrum of bacteria, including *E. coli*, *S. aureus*, and *Pseudomonas aeruginosa*. MOFs can produce ROS under light, damaging bacterial structure, leading to cell content leakage and bacterial death. This ROS generation boosts their efficacy, especially against resistant strains. However, MOFs' practical use is constrained by stability issues in humid environments, affecting performance and recovery. The powder form also presents recovery challenges and toxicity risks. The synthesis of most MOFs is complex and costly, often requiring high-pressure, high-temperature hydrothermal/solvothermal methods. Future research should emphasize green synthesis for decreased energy usage. Further investigation is required to explore the biosafety of MOFs, particularly their long-term toxicity, side effects, and metabolic product toxicity. Moreover, the limited light penetration restricts the use of MOFs that produce heat and ROS under light. Developing MOF-based materials responsive to longer wavelength energy is essential for broader medical applications.

### 3.5. MXenes

MXenes, a unique class of two-dimensional materials derived from MAX phases, are synthesized primarily by selectively etching the A element, typically a group 13 or 14 element [54]. The resulting 2D materials are transition metal carbides, nitrides, or carbonitrides, which exhibit exceptional photocatalytic and antibacterial properties due to their ability to generate ROS under light exposure. These ROS are instrumental in disrupting bacterial cells, making MXenes potent agents against various pathogens. The antibacterial properties of MXenes are attributed to their ability to physically harm bacterial cells, generate oxidative stress, and produce both photothermal and photodynamic effects. These diverse mechanisms are especially potent against bacterial pathogens, positioning MXenes as promising contenders for various antibacterial uses. The surface functionalities like -OH, -F, and -O groups enhance the materials' hydrophilicity, which promotes better water adsorption, facilitating the formation and diffusion of ROS in aqueous environments. The slow charge dynamics of single semiconductor photocatalysts significantly hinder the generation

of ROS. In composite materials, charge migration follows random diffusion, which greatly inhibits charge dynamics. The Fermi level of  $\text{Ti}_3\text{C}_2\text{X}$  is  $-0.05\text{ V}$ , more positive than the conduction band of most n-type semiconductors, indicating its potential as a cocatalyst for transferring and accumulating photogenerated electrons. To accelerate interfacial charge dynamics and promote ROS generation, Liu et al. proposed an interfacial engineering strategy based on work function theory [55] (Figure 7). This strategy induces an internal electric field (IEF) in the lamellar  $\text{Ti}_3\text{C}_2\text{Tx}/\text{TiO}_2$  composite material, thereby enhancing photocatalytic bactericidal performance. DFT calculations help understand the electronic structure of photocatalysts by predicting how these materials interact with bacterial components, revealing potential reaction sites and energy levels critical for effective photocatalysis. DFT calculations and in-situ irradiated X-ray photoelectron spectroscopy (ISI-XPS) results indicate that the IEF enables directional separation of photogenerated carriers. Efficient charge dynamics favor ROS generation, leading to excellent broad-spectrum bactericidal performance. Different work function values of  $\text{Ti}_3\text{C}_2\text{Tx}$  and  $\text{TiO}_2$  induce an internal electric field at the interface. Under visible light irradiation, electrons generated by  $\text{TiO}_2$  are driven by the IEF to  $\text{Ti}_3\text{C}_2\text{Tx}$ , catalyzing the formation of  $\cdot\text{O}_2^-$ . Meanwhile, holes left in the valence band of  $\text{TiO}_2$  react with water to produce hydroxyl radicals  $\cdot\text{OH}$ . The high bactericidal activity mechanism is attributed to the enhanced ROS generation facilitated by accelerated carrier separation and directional transfer at the interface. Additionally, following five repeated photocatalytic bactericidal tests, the  $\text{Ti}_3\text{C}_2\text{Tx}/\text{TiO}_2$  immobilized on insoluble polylactic acid (PLA) maintained a sterilization efficiency of 99%.

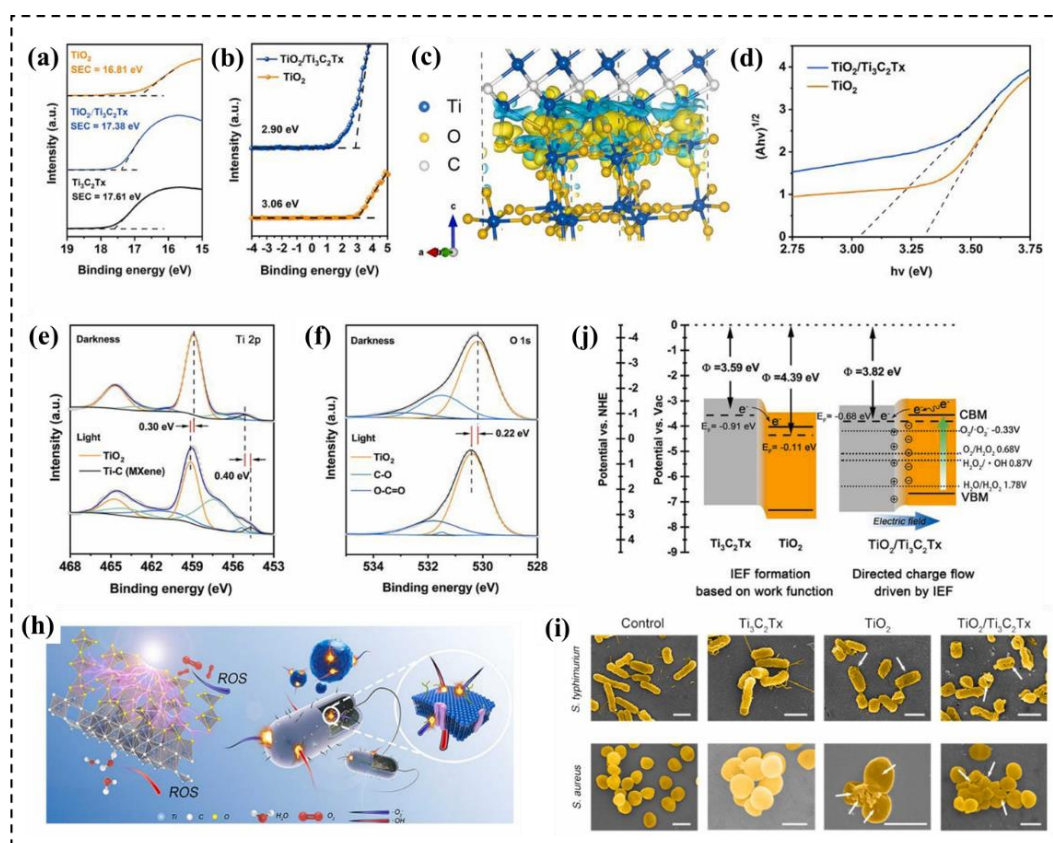


**Figure 7.** The mechanism of work function mediated interface charge kinetics. (a) UPS spectra of  $\text{Ti}_3\text{C}_2\text{Tx}$ ,  $\text{TiO}_2$ , and  $\text{Ti}_3\text{C}_2\text{Tx}/\text{TiO}_2$ ,  $h\nu = 21.20\text{ V}$ . (b) Valence band XPS of  $\text{TiO}_2$  and  $\text{Ti}_3\text{C}_2\text{Tx}/\text{TiO}_2$ . (c) Charge density difference of  $\text{Ti}_3\text{C}_2\text{Tx}/\text{TiO}_2$ . Cyan and yellow areas represent electron depletion and accumulation, respectively. (d) Tauc plots of  $\text{TiO}_2$  and  $\text{Ti}_3\text{C}_2\text{Tx}/\text{TiO}_2$  obtained from UV-vis DRS. (e, f) ISI-XPS spectra of Ti 2p and O 1s of  $\text{Ti}_3\text{C}_2\text{Tx}/\text{TiO}_2$ . (g) The scheme of electric field formation based on work function, and steers interface charge kinetics by the electric field. (h) Schematic illustration of steering interface charge kinetics based on work function for boosting visible light photocatalytic sterilization. (i) SEM images exhibit the morphology of *S. typhimurium* and *S. aureus* after incubating with  $\text{Ti}_3\text{C}_2\text{Tx}$ ,  $\text{TiO}_2$ , and  $\text{Ti}_3\text{C}_2\text{Tx}/\text{TiO}_2$  under light illumination. Ref. [55] reproduced with permission. Copyright 2023, Elsevier.

The antibacterial mechanisms of MXenes are primarily attributed to the physical disruption of bacterial membranes due to their sharp edges and the generation of ROS, leading to oxidative stress in bacterial cells, and causing cell lysis. Their high surface area, excellent conductivity, and the ability to generate ROS contribute to their broad-spectrum antibacterial activity against many bacteria, including antibiotic-resistant strains such as

*Methicillin-resistant Staphylococcus aureus* and *Vancomycin-resistant Enterococci*. Mxenes possess photothermal properties that enable them to kill bacteria effectively when exposed to near-infrared light, broadening their application in antibacterial textiles and coatings. However, the potential cytotoxicity and long-term biocompatibility of Mxenes are significant concerns that require thorough investigation to ensure safe biomedical applications. Additionally, the challenges associated with large-scale production of Mxenes with consistent quality and morphology must be addressed to enhance their commercial viability and application potential.

#### 4. The Influencing Factors of Photocatalytic Antibacterial Efficacy

##### 4.1. The Influence of Environmental Factors on the Photocatalytic Antibacterial Efficacy

###### 4.1.1. pH Value

The impact of pH on the photocatalytic process can be outlined as follows: (a) Modulating surface charge to affect the adsorption capacity of target pollutants; (b) Changing the ROS generation rate in the photocatalytic system; (c) Affecting the stability of the catalyst. ROS and the adsorption of microorganisms are influenced by the charge distribution on the surface of photocatalysts, which is influenced by the pH of the solution [56]. The surface charge of photocatalysts such as ZnO, CuO, and TiO<sub>2</sub> is influenced by pH levels. At different pH levels, the surface properties of these photocatalysts change, thereby altering their interaction with bacterial cells. Under acidic conditions, the surface of these catalysts typically carries a positive charge, which can attract and destabilize negatively charged bacterial cell membranes. Conversely, under basic conditions, the surface becomes negatively charged, which might repel bacterial cells, thus reducing the photocatalyst's bactericidal efficiency [57]. The generation and effectiveness of ROS can be pH-dependent. For example, at higher pH levels, the increased generation of •O<sub>2</sub><sup>-</sup> can enhance microbial cell wall damage. Moreover, the interaction between the generated ROS and the bacterial cells can be facilitated or hindered based on the pH-induced changes in bacterial surface properties [58,59]. The pH can also influence the stability and dissolution of photocatalysts. Certain photocatalysts may dissolve at extreme pH values, releasing metal ions that have additional antimicrobial effects. However, excessive dissolution might lead to loss of photocatalytic activity and hence decreased overall antimicrobial performance. Understanding the stability of photocatalysts across different pH levels is crucial for their effective application in antibacterial coatings or water treatment systems [60].

###### 4.1.2. Temperature

Increasing the temperature can enhance photocatalytic reactions by facilitating the movement of charge carriers within the photocatalyst. This acceleration is attributed to the promotion of mobility for charge carriers. This facilitates the generation of ROS, which are crucial for efficiently and rapidly deactivating bacteria. Meanwhile, elevated temperatures slow down the rate at which electron-hole pairs recombine, increasing the total quantum efficiency of photocatalysts like TiO<sub>2</sub> and g-C<sub>3</sub>N<sub>4</sub> in the breakdown of organic pollutants like Congo Red [61]. High temperatures typically boost the energy available for overcoming the activation barriers of photocatalytic reactions, thus enhancing the generation of these potent antimicrobial agents [62]. Higher temperatures may disrupt microbial cell membranes, making them more permeable and vulnerable to oxidative stress induced by photocatalytic reactions. This makes bacterial populations more susceptible to destruction under photocatalytic conditions [63]. Reactants and bacteria adsorb differently on photocatalyst surfaces depending on temperature. High temperatures can potentially enhance the frequency of interaction between the catalyst and target bacteria, potentially enhancing the interaction frequency between the catalyst and target bacteria, thereby increasing the rate of microbial inactivation [57].

###### 4.1.3. Light Intensity

Photocatalysts function by absorbing light to activate their surface, leading to the production of ROS. Because of their extreme reactivity, these ROS can break down bacterial cell walls, rendering the bacterium inactive or lethal. The intensity of the light source has a major impact on the efficiency of ROS generation and, in turn, the antibacterial activity of photocatalysts. A critical study of Bi<sub>2</sub>WO<sub>6</sub>-based heterojunction photocatalysts discusses the optimization of these materials for environmental applications. These photocatalysts can function under lower light intensities compared to traditional TiO<sub>2</sub>, because of their extended absorption into the visible light spectrum and efficient charge carrier separation. The photocatalytic degradation efficiency of organic pollutants and microbial pathogens is significantly enhanced by increased light intensity up to a certain threshold, attributing this

improvement to the enhanced charge carrier generation which increases ROS production [64]. Further reinforcing these findings, *G. Lofrano* discussed the antimicrobial effectiveness of innovative photocatalysts designed to operate under visible light. The research indicated that engineered photocatalysts that harness visible light show increased antibacterial activity as the light intensity escalates, which supports their use in real-world environmental conditions where solar light is the primary energy source. Moreover, the interplay between photocatalyst material properties, light intensity, and microbial inactivation kinetics is detailed in a study by *D. Sapińska*. The research explores the dynamics of photocatalytic degradation and reveals that higher light intensities expedite the photocatalytic reactions by providing more energy for the excitation of electrons in the photocatalyst material. This energy boost enhances the overall efficiency of microbial disinfection processes [59].

#### 4.1.4. Humidity

Photocatalysts rely on their interaction with the environment to produce ROS that are essential for their antibacterial activity. Humidity, specifically the presence of water vapor, plays a significant role in the generation and effectiveness of ROS. High humidity conditions enhance the photocatalytic reactions by increasing the availability of water molecules, which are necessary for the formation of  $\bullet\text{OH}$  and other ROS. Water molecules adsorbed onto the surface of photocatalysts, such as  $\text{TiO}_2$ , participate in redox reactions upon light activation, leading to the production of  $\bullet\text{OH}$ . These hydroxyl radicals are highly effective in breaking down bacterial cell walls and inactivating microorganisms. The role of humidity in this process is crucial as it directly influences the availability and mobility of water molecules on the photocatalyst surface. Higher humidity levels can significantly improve the antibacterial efficiency of photocatalysts. A study on  $\text{TiO}_2$  photocatalysts revealed that their antibacterial activity against *E. coli* was enhanced in humid environments due to the increased generation of  $\bullet\text{OH}$  radicals [65]. This enhancement is attributed to the higher adsorption of water molecules on the photocatalyst surface, which facilitates the redox reactions necessary for ROS production. The presence of humidity not only aids in the generation of ROS but also affects their stability and diffusion. High humidity levels help maintain a hydrated environment, which prevents the rapid recombination and decomposition of ROS, thereby prolonging their antimicrobial action.

#### 4.1.5. Organic Matter

Photocatalysts function by absorbing light to activate their surface, leading to the production of ROS. Because of their extreme reactivity, these ROS can break down bacterial cell walls, rendering the bacterium inactive or lethal. The presence of organic matter in the environment significantly impacts the effectiveness of photocatalytic antibacterial activity. Organic matter can interact with the photocatalyst and the generated ROS, influencing the overall efficiency of the disinfection process. In a study involving  $\text{TiO}_2$  nanoparticles, it was observed that the increase in organic matter concentration from 0% to 100% resulted in an 85% decrease in microbicidal efficacy against *E. coli* [66]. This reduction is primarily due to the competition between organic matter and bacteria for ROS, particularly  $\bullet\text{OH}$ , which is crucial for the bactericidal action of photocatalysts. The impact of organic matter can be attributed to several factors. Turbidity caused by organic matter can hinder light penetration, reducing the activation of the photocatalyst. Additionally, organic compounds, such as phenolics, can act as scavengers for ROS, thereby reducing the availability of these species for bacterial inactivation. Experimental evidence suggests that increasing the total phenolics content in the medium from 20 to 114 mg/L decreases the log reduction of *E. coli* from 2.7 to 0.38 CFU/mL. Similarly, an increase in protein content from 0.12 to 1.61 mg/L decreases the log reduction from 5.74 to 0.87 CFU/mL. Theoretical calculations and experimental observations support these findings. The presence of phenolic compounds and proteins in the suspension medium can form complexes with the photocatalyst surface, inhibiting the generation of ROS and their subsequent interaction with bacterial cells. This phenomenon underscores the need for careful consideration of organic matter when applying photocatalytic materials in real-world environments, such as food processing or wastewater treatment.

#### 4.1.6. Environmental Medium

The medium in which photocatalysts operate significantly influences their antibacterial activity by affecting the generation and stability of ROS. Studies have shown that different ions present in the suspension medium, such as chloride and phosphate, can alter the properties of nanoparticle suspensions, including their stability and ROS production. A research on  $\text{TiO}_2$  and  $\text{ZnO}$  nanomaterials has demonstrated that the antibacterial and photocatalytic activities are highly dependent on the composition of the medium [67]. The presence of chloride and phosphate ions in the medium can distinctly affect the photocatalytic process. In phosphate buffer solutions,  $\text{TiO}_2$  and  $\text{ZnO}$  nanoparticles exhibit different behaviors compared to saline solutions. The stability of the

nanoparticle suspension and the release of metal ions are significantly influenced by these ions, impacting ROS production and overall antibacterial activity. TiO<sub>2</sub> nanoparticles tend to form larger aggregates in saline solutions, while in phosphate buffer solutions, they form more stable dispersions. This stability in phosphate solutions enhances the photocatalytic generation of ROS. Theoretical calculations and experimental observations suggest that phosphate ions can suppress the generation of superoxide ions in TiO<sub>2</sub> suspensions while enhancing the production of •OH radicals. This suppression and enhancement can be attributed to the interactions of phosphate ions with the nanoparticle surfaces, which influence the transfer of photogenerated holes and electrons. In contrast, chloride ions do not significantly affect ROS generation, making saline solutions less effective in enhancing photocatalytic antibacterial activity compared to phosphate buffers. Further studies have highlighted the importance of medium composition on the antibacterial effectiveness of ZnO nanoparticles. In phosphate buffer solutions, ZnO nanoparticles exhibit reduced antibacterial activity due to the formation of zinc phosphate precipitates, which lower the availability of Zn<sup>2+</sup> ions. These ions are crucial for the toxicity of ZnO nanoparticles, as they contribute to ROS generation and direct interactions with bacterial cells. The reduction in Zn<sup>2+</sup> ion concentration in phosphate buffers decreases the ROS production, thereby lowering antibacterial activity.

#### 4.2. Design Strategies for Improving Photocatalytic Antibacterial Performance

##### 4.2.1. Doping

Doping is a widely utilized technique to extend the light response range of materials, particularly in the fields of semiconductors, photocatalysts, and solar cells. Doping involves adding a small amount of impurity atoms to a pure semiconductor. Impurity atoms can act as either donors, providing extra electrons, or as acceptors, creating holes by accepting electrons. When dopants are introduced into a semiconductor, they create new energy levels within the band gap. Dopants can introduce sub-bandgap states, enabling the absorption of photons with energies lower than the intrinsic band gap. The phenomenon of sub-band gap absorption holds great potential for utilizing visible light in photocatalysis. The generation efficiency of ROS is reduced by fast electron-hole pair recombination, which poses significant barriers to photocatalytic disinfection efficacy. To combat this issue, various techniques have been devised to enhance the separation and movement of charge carriers. Doping ZnO with low-concentration fluorine enhances its photocatalytic and antibacterial properties, as well as the mobility of ROS carriers in non-UV environments. By using a sol-gel method, Joanna et al. [68] created fluorine-doped nanoparticulate ZnO powder and investigated how this technique affected ZnO's antibacterial activity against particular pathogens in the presence of light. Since F-doping produces reactive oxygen species and the particles are nanosized, ZnO photocatalysts have enhanced antibacterial activity against *S. aureus* (99.99%) and *E. coli* (99.87%). In addition, doping with 10% Cu<sup>2+</sup> in MOFs leads to a 99.71% antibacterial efficacy against *S. aureus* within 20 min. Cu<sup>2+</sup> was included in the MOFs by Han et al. [51] to obtain improved photocatalytic activities and photothermal effects. This effectively reduced the recombination of photogenerated electron-hole pairs and increased light absorption through the Cu<sup>2+</sup> d-d transition, finally enhancing the generation and utilization of ROS. MOF's porphyrin ring's capacity for photocatalysis and photothermal reactions is improved by adding Cu<sup>2+</sup>. Cu<sub>10</sub>MOF showed the best performance. Excessive Cu<sup>2+</sup> reduces both abilities, as in Cu<sub>25</sub>MOF, which performed the worst. The results of the photocurrent response showed that when exposed to light, Cu<sub>10</sub>MOF produced the greatest number of electrons, suggesting the fastest rate of electron and hole separation. Cu<sub>15</sub>MOF, Cu<sub>5</sub>MOF, MOF, and lastly Cu<sub>25</sub>MOF came after this (Figure 8).

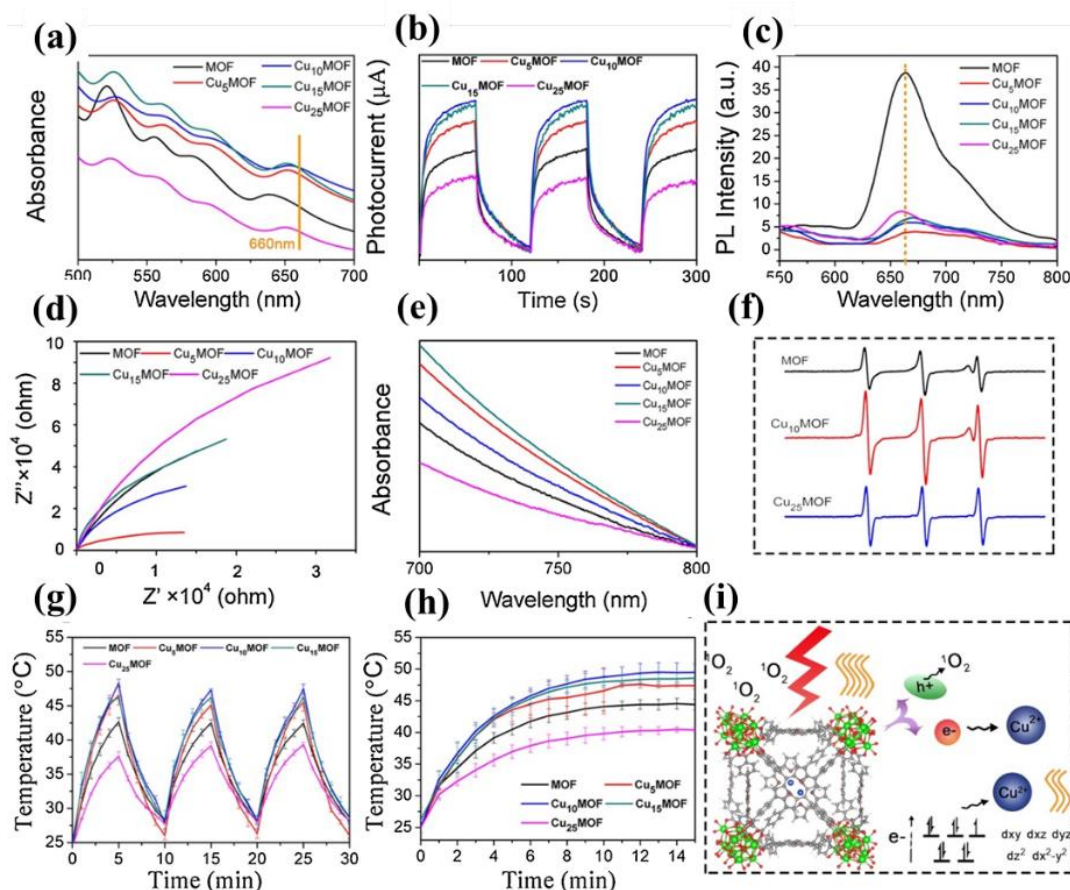


**Figure 8.** (a) UV–vis absorption spectra of MOF, Cu<sub>5</sub>MOF, Cu<sub>10</sub>MOF, Cu<sub>15</sub>MOF, Cu<sub>25</sub>MOF solution at the same concentration; (b) photocurrent responses; (c) PL spectra; (d) EIS Nyquist plots; (e) The lower-energy edge of the corresponding UV–vis absorption profiles; (f) ESR of MOF, Cu<sub>5</sub>MOF, Cu<sub>10</sub>MOF, Cu<sub>15</sub>MOF, Cu<sub>25</sub>MOF; (g) Temperature rising and cooling profiles; (h) Photothermal curves of MOF, Cu<sub>5</sub>MOF, Cu<sub>10</sub>MOF, Cu<sub>15</sub>MOF, Cu<sub>25</sub>MOF (500 ppm) when irradiation with 660 nm light is turned on/off (0.4 W/cm<sup>2</sup>); (i) schematic illustration of the mechanism of enhanced photocatalytic and photothermal ability of Cu<sup>2+</sup> doped MOFs. Ref. [51] reproduced with permission. Copyright 2020, Elsevier.

#### 4.2.2. Noble Metal Deposition

Precious metals like Au, Ag, and platinum can exhibit localized surface plasmon resonance (LSPR) when exposed to light. LSPR significantly enhances the electromagnetic field near the metal surface, leading to increased light absorption in the visible and near-infrared regions. This effect broadens the light absorption range of the photocatalyst, enabling it to utilize more of the solar spectrum. Besides, Precious metals can act as electron sinks, rapping photogenerated electrons and facilitating their participation in redox reactions that generate ROS. Upon light absorption, electrons in the semiconductor are excited from the valence band to the conduction band, leaving behind holes. The precious metal deposits can capture these electrons, preventing them from recombining with holes. This extended lifetime of charge carriers increases the probability of their participation in redox reactions, thereby enhancing photocatalytic efficiency. He et al. [69] reported Au nanoparticles deposited on ZnO nanostructures significantly enhance their photocatalytic and antibacterial activity, even at a minimal Au/ZnO molar ratio of 0.2%, there is a substantial boost in the photocatalytic and antibacterial capabilities of ZnO, showing promise for applications in water treatment and antibacterial products. Stronger adsorption below 350 nm and an absorption edge shift to shorter wavelengths were seen in the UV-vis spectra of ZnO suspensions both before and after treatment with Au dots. Increased ROS production and photocatalytic activity may result from the following possible effects of Au in ZnO/Au hybrid nanostructures: (1) amplified light absorption due to Au’s surface photoluminescence; (2) modification of ZnO’s band gap, which would increase the reactivity of photoinduced charge carriers; and (3) improved electron transport and charge carrier separation efficiency.



#### 4.2.3. Morphology Control

Morphology control is a crucial strategy to expand the light absorption range and improve the photocatalytic efficiency of materials. By optimizing the shape, size, and structure of photocatalysts, it is possible to enhance light absorption, improve charge separation, and increase catalytic activity. The photocatalyst with a small specific surface area has limited light contact, reducing light absorption. Furthermore, the insufficient specific surface area fails to provide enough active sites for photocatalytic reactions, resulting in a lower rate of ROS utilization. Therefore, controlling the morphology can enhance the specific surface area of the photocatalyst, broaden the light absorption range, and improve its ability to generate ROS. Ultimately, this will enhance the photocatalytic efficiency of the photocatalyst. Nanostructures can improve light trapping and increase the likelihood of light absorption within the material. Nanoparticles, nanorods, and nanotubes can significantly increase the surface area of the photocatalyst, allowing for enhanced light absorption and a greater number of active sites available for photocatalytic reactions. A unique CdS/Ti<sup>3+</sup>/N-TiO<sub>2</sub> (TNTC) nanorod composite photocatalyst was created by Qin et al. [70], its high specific surface area offers a large number of active reaction sites for photocatalysis. By creating an internal electric field, the CdS and TNT heterojunctions effectively enhance the spatial segregation of photogenerated carriers, ultimately amplifying the efficiency of photocatalytic reactions. Furthermore, hierarchical structures such as mesoporous or hollow spheres can confine light within the structure, thereby increasing the optical path length and enhancing light absorption.

#### 4.2.4. Vacancy Introduction

Introducing vacancies is a powerful method to regulate the bandgaps and improve the photocatalytic antimicrobial efficiency of semiconductors. The interaction between the defect states and the conduction or valence bands, effectively reducing the energy required for electron excitation, leads to bandgap narrowing by altering the material's electronic structure. Vacancies can act as traps for electrons or holes, which reduces the recombination rate of photogenerated charge carriers. By trapping electrons or holes, vacancies extend the lifetime of these charge carriers. This prolonged charge separation leads to more effective generation of ROS, especially •OH and •O<sub>2</sub><sup>-</sup>, greatly improving the antibacterial efficiency of photocatalysis. Defect engineering strategies are in high demand to effectively adjust the electronic microstructure and surface morphologies of semiconductors to increase charge carrier concentration and regulate bandgaps. Jin et al. [71] effectively used the reflux approach to create a nanostructured caged Iodine-modified ZnO (I-ZnO-n) catalyst with a surface oxygen vacancy. The antibacterial capabilities of caged iodine-modified ZnO nanoparticles are superior to those of micron-structured ZnO due to their increased surface oxygen vacancy and improved photogenic carrier separation efficiency. An increased ability of the oxygen vacancy to separate photo-excited charge carriers results in a large increase in the number of free radicals produced. Higher concentrations of oxygen vacancies accelerate the pace of bacterial inactivation.

#### 4.2.5. Heterojunction

The bandgap of a photocatalyst is a fundamental property that dictates its ability to absorb light and generate ROS. Energy band regulation in photocatalysts is a critical strategy for enhancing their photocatalytic activity. A wide band gap constrains the photocatalytic activity due to the absorption of fewer photons and the subsequent generation of fewer reactive species. Conversely, a very narrow band gap in photocatalysts can lead to enhanced absorption of visible light, potentially increasing photocatalytic activity under broader lighting conditions. On the other hand, a key disadvantage of an overly narrow band gap is the possibility for swift recombination of the photogenerated electron-hole pairs. Rapid recombination might drastically reduce the efficiency of the photocatalyst, as it leaves fewer charge carriers to engage in the photocatalytic processes, therefore limiting ROS production. The formation of heterojunctions often results in nanostructured materials with increased surface area and more active sites, which can adsorb and activate more reactant molecules, facilitating the generation and diffusion of ROS. Two semiconductors with staggered band alignments are combined in a type II heterojunction. This arrangement creates an interface where the CB of one semiconductor is lower in energy than the CB of the other, and similarly, the valence band VB of one is higher than the VB of the other. Electrons in the higher-energy CB can transfer to the lower-energy CB, while holes in the higher-energy VB move to the lower-energy VB. This effectively reduces the bandgap and allows for more efficient absorption of visible light, thereby broadening the light absorption range. The Z-scheme heterojunction imitates the natural photosynthetic process. It involves the direct transfer of photogenerated electrons from the CB of one semiconductor to the VB of another, preserving the high redox potential of the electrons and holes. This type of heterojunction maintains a high oxidative and reductive ability, enhancing the photocatalytic performance under visible light. The Z-scheme structure helps in utilizing a

broader spectrum of sunlight, effectively regulating the bandgap. Shi et al. [72] successfully prepared a highly efficient  $\text{CuBi}_2\text{O}_4/\text{Bi}_2\text{MoO}_6$  p-n heterojunction.  $\text{CuBi}_2\text{O}_4/\text{Bi}_2\text{MoO}_6$  exhibited enhanced photocatalytic efficacy for eradicating *E. coli*, with near-complete inactivation in 4 h. The improved photocatalytic performance was linked to the creation of a p-n heterojunction, while the presence of  $\text{Cu}^{2+}$  had little impact on the elimination of *E. coli*. When forming a heterojunction, the conduction band of  $\text{Bi}_2\text{MoO}_6$  and the valence band of  $\text{CuBi}_2\text{O}_4$  were elevated, leading to a heightened redox capacity. The internal electric field within the heterojunction plays a crucial role in enhancing the spatial dispersion and movement of the photogenerated hole-electron pairs. This, in turn, enhances visible light absorption, leading to the production of more active substances such as  $\text{h}^+$ ,  $\text{e}^-$ , and  $\bullet\text{O}_2^-$ . These substances can destroy the DNA and proteins of bacteria and promote their death. These strategies not only enhance the photocatalytic efficiency but also make the process more energy-efficient and sustainable.

#### 4.2.6. Cocatalysts

Cocatalysts play a crucial role in enhancing the efficiency of photocatalytic processes. They accelerate electron cycling and reduce the recombination of electron-hole pairs. Metal cocatalysts such as Pt, Au, and Ag can serve as electron sinks, trapping excited electrons in the conduction band of the photocatalyst. By trapping these electrons, metallic cocatalysts prevent them from recombining with holes in the valence band. Cocatalysts create a favorable environment for charge separation by forming Schottky barriers at the interface with the photocatalyst, which efficiently separate electron-hole pairs. Cocatalysts also improve the transfer of electrons to molecular oxygen, forming  $\bullet\text{O}_2^-$ , which can further react to form  $\bullet\text{OH}$  and  $\text{H}_2\text{O}_2$ . Using a simple solvothermal method, Jin et al. [73] synthesized an innovative  $\text{TiO}_2/\text{W}_{18}\text{O}_{49}/\text{MXene}$  (TWM) ternary composite with dual electronic transmission channels. The TWM composite has a significantly higher sterilization rate than TM, at 93.7%. The findings demonstrate that practically all bacteria were destroyed upon light exposure, demonstrating the TWM composite's superior antibacterial qualities under light. This is mostly because the cocatalyst modification and Z-scheme heterojunction work together. ROS are produced at a higher rate during photocatalytic electron-hole separation and electron transfer caused by two electronic transmission channels in the Schottky junction and Z-scheme heterojunction. Furthermore, the MXene cocatalyst functions as a support matrix by increasing the number of surface-active sites, improving light absorption, and boosting charge separation efficiency. These actions successfully encourage the production of ROS and ultimately improve the catalytic performance of the  $\text{TiO}_2/\text{W}_{18}\text{O}_{49}/\text{MXene}$  ternary material.

#### 4.2.7. Surface Functionalization

Functionalizing photocatalysts with functional groups such as -OH, -NH<sub>2</sub>, or -COOH can introduce new surface active sites. This enhances interactions with reactants and facilitates electron transfer, thereby accelerating the diffusion of ROS. These modifications contribute to the overall improvement in photocatalytic activity. The use of organic molecules for such modifications has been extensively studied and proven effective in enhancing electron cycling. Organic molecules reduce surface recombination sites and act as passivation layers, effectively preventing semiconductor photo-corrosion. In addition, organic compounds, including metal and non-metal complex dyes, are used as photosensitizers for semiconductors with broad bandgaps. When exposed to light, electrons excited by the dyes attached to the semiconductor surface are transferred into the semiconductor's conduction band. At the same time, the dye molecules, having lost electrons, can be replenished by accepting electrons from electron donors. To develop an antibacterial substance based on g-C<sub>3</sub>N<sub>4</sub> for photocatalytic treatment, it is necessary to broaden the light absorption spectrum of g-C<sub>3</sub>N<sub>4</sub> and strengthen its interaction with bacteria, Guo et al. [74] grafted acridinium (ADN) groups onto g-C<sub>3</sub>N<sub>4</sub> nanosheets. By coupling ADN into the g-C<sub>3</sub>N<sub>4</sub> skeleton, the  $\pi$ -conjugated ADN can alter the electronic structure of g-C<sub>3</sub>N<sub>4</sub> by causing a narrow optical band gap and a wide optical absorption spectrum spanning from UV to NIR. This significantly increases ROS production and photocatalytic activity. The output of  $\bullet\text{OH}$  and  $^1\text{O}_2$  generated by acridine in the presence of O<sub>2</sub> and H<sub>2</sub>O is significantly increased by grafting ADN. According to the findings, the predominant reactive oxygen species during the photocatalysis of g-C<sub>3</sub>N<sub>4</sub> and ADN@g-C<sub>3</sub>N<sub>4</sub> are  $^1\text{O}_2$ ,  $\bullet\text{OH}$ , and  $\bullet\text{O}_2^-$ . When produced ROS come into touch with planktonic bacteria directly, they may spread into bacterial suspensions and cause structural damage. Molecular dynamics simulations provide valuable insights into the interaction between photocatalysts and bacterial membranes. This helps us understand how photocatalysts disrupt bacterial membranes at a molecular level, which can help us model the dynamics of photocatalytic reactions and predict potential antibacterial pathways. According to molecular dynamics simulations, ADN@g-C<sub>3</sub>N<sub>4</sub> can migrate via strong van der Waals and electrostatic contacts toward, orient into, and enter into bacterial lipid bilayer membranes. This procedure improves ROS movement while decreasing lipid orderliness, which gives ADN@g-C<sub>3</sub>N<sub>4</sub> enhanced antibacterial and antibiofilm properties.

## 5. Photocatalysts in Antimicrobial Applications

### 5.1. Purification of Drinking Water

Recent research has focused on improving the practical deployment of photocatalysts in water purification. Innovations include developing floatable and water-durable photocatalytic materials, like TiO<sub>2</sub>-coated nets, designed for easy application in bodies of water, including in remote and developing regions. These systems leverage the low-cost and sustainable aspects of solar energy, offering a viable solution to waterborne diseases prevalent in such areas. Wang et al. [75] investigated a BiVO<sub>4</sub>/graphene oxide multifunctional hydrogel for water purification. The hydrogel enhances photocatalytic activity by interfacial adsorption-enrichment mechanisms that increase the local concentration of contaminants around the photocatalyst, thereby improving the ROS generation efficiency. SEM provides detailed images of morphological changes in photocatalysts and bacteria during interaction, facilitating visualization of the impact of photocatalysts on bacterial cell structures (Figure 9). Photocatalyst-activated ROS can penetrate *E. coli* cells and overpower their antioxidant systems, causing protein oxidation. Oxidative stress impairs bacterial cell membrane enzymes, leading to loss of cell function, degeneration, and death. This method addresses the limitations of TiO<sub>2</sub> by utilizing visible light, which is more abundant in natural sunlight. Izuma et al. [76] developed a floatable, water-durable TiO<sub>2</sub>-coated net with enhanced photocatalytic antibacterial properties. The net is designed for use in developing countries, providing a practical and cost-effective solution for water purification. The TiO<sub>2</sub> coating on the net remains active under solar irradiation, continuously generating ROS that purify water by decomposing organic contaminants and inactivating pathogens. Yang's research [77] introduced magnetic photocatalytic antimicrobial materials (MPAMs) that facilitate easy recovery and reuse of the photocatalysts. These materials combine the antibacterial properties of photocatalysis with the convenience of magnetic separation, making the water treatment process more efficient and sustainable. The MPAMs utilize a dual mechanism where the magnetic core allows for easy collection, while the photocatalytic shell actively purifies water. The application of photocatalytic antimicrobials in water disinfection represents a significant advancement in public health protection. Continuous innovations in material science and engineering are expected to further enhance the effectiveness and applicability of these systems, making clean and safe water more accessible worldwide. The ongoing development of new photocatalytic materials and configurations promises to address the current limitations and expand the utility of this technology in sustainable water management.

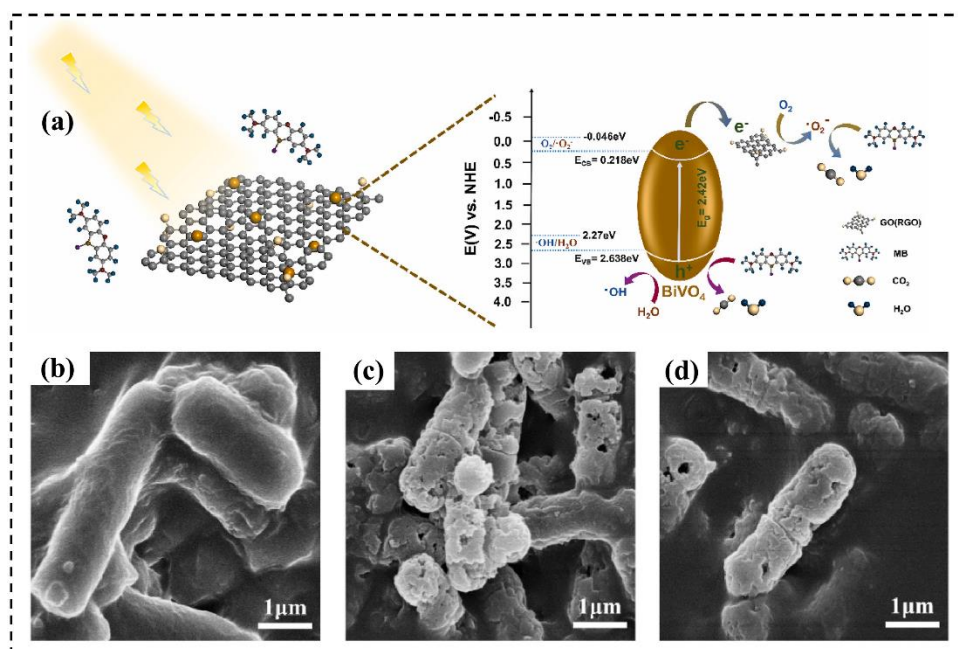


**Figure 9.** (a) Schematic illustration of the photocatalytic mechanism for the BV-GH composite; (b) SEM images for Normal *E. coli*; (c,d) SEM images for *E. coli* inactivated by the BV-GH<sub>2</sub> composite treatment. Ref. [75] reproduced with permission. Copyright 2022, Elsevier.

### 5.2. Medical Equipment and Antimicrobial Coatings

In the medical sector, photocatalytic materials are increasingly applied, particularly as coatings on medical devices to curb the proliferation of hospital-acquired infections. The antimicrobial properties of TiO<sub>2</sub> enable the creation of surfaces capable of inactivating various bacteria, including strains resistant to antibiotics such as MRSA. The underlying mechanism of this photocatalytic inactivation involves ROS production, which disrupts the bacterial cell wall and membrane, ultimately causing cell demise. Photocatalytic coatings [78] have proven effective on diverse medical devices, including catheters, surgical instruments, and implants, thereby diminishing infection risks and enhancing patient outcomes. Yao's study [79] utilized TiO<sub>2</sub> nano-particles embedded in complex structures to increase surface area and ROS production, significantly enhancing bacterial inactivation on medical surfaces. F. Ubaldi [80] emphasized the development of nanostructured surfaces that enhance photocatalytic efficiency under visible light. This approach addresses one of the main limitations of traditional photocatalytic materials—the requirement for UV light—making them more applicable in indoor environments where UV exposure is limited. Integration of photocatalytic coatings in medical devices can effectively reduce nosocomial infections. These coatings are applied to high-contact surfaces such as surgical tools, bed rails, and other hospital equipment to continuously disinfect them by degrading microbial agents present. The systematic review by H. Qiu provides a comprehensive analysis of different antimicrobial polymers used in photocatalytic coatings, highlighting their advantages in preventing bacterial growth on medical devices [81]. Despite significant advancements, several challenges remain. The photocatalytic activity can be inhibited by the presence of organic matter, which is abundant in medical environments. Moreover, the stability and potential toxicity of nanoparticle-based photocatalysts under long-term use are still under scrutiny.

### 5.3. Air Purification

Photocatalytic materials are also employed in air purification [82], a promising application given the increasing concerns over indoor air quality. This stems from the prevalence of VOCs and airborne pathogens. Photocatalysts such as TiO<sub>2</sub> and ZnO are integrated into air purifiers and building materials to decompose VOCs and neutralize airborne microorganisms. The photocatalytic process eradicates harmful pollutants and mitigates odors and allergens, contributing to a healthier indoor atmosphere. The integration of diverse photocatalytic technologies underscores a concerted effort to enhance air purification methods across varying environmental conditions. Research by Wang et al. [83] demonstrates that Air filters made from ZIF-8 have demonstrated exceptional effectiveness in combatting pollution, boasting a photocatalytic lethality rate of over 99.99% against airborne bacteria within just 30 min, along with a 97% removal rate of particulate matter. Research focusing on mechanisms has uncovered that photoelectrons captured by zinc centers in ZIF-8 through ligand-to-metal charge transfer are accountable for generating ROS linked to oxygen reduction, thereby serving as the primary disinfection process. Besides, Dong and colleagues [84] employ Ca-intercalated g-C<sub>3</sub>N<sub>4</sub> as a prototype photocatalyst to investigate the processes involved in photocatalytic elimination of NO. The introduction of Ca creates surplus localized electrons, which, under visible light, form electron-hole pairs captured by gas molecules. This produces additional ROS and initiates chemical reactions. Compared to unmodified g-C<sub>3</sub>N<sub>4</sub>, Ca-doped g-C<sub>3</sub>N<sub>4</sub> generates ROS with higher oxidation potential, enhancing photocatalytic NO oxidation, reducing activation energies, improving NO removal efficiency, and lowering NO<sub>2</sub> formation. This study introduces an innovative method to achieve effective and safe air purification.

## 6. Conclusion and Outlook

The extensive research and development in photocatalytic antibacterial technology have paved the way for innovative strategies to tackle the global challenge of antimicrobial resistance. This review summarises the process and mechanism of •OH, •O<sub>2</sub><sup>-</sup>, <sup>1</sup>O<sub>2</sub>, and H<sub>2</sub>O<sub>2</sub> generation in photocatalytic reactions, focusing on the research progress of different common photocatalytic bactericides and modification strategies of photocatalysts. The review also examines the environmental factors that affect the antibacterial efficacy of photocatalysis. Various approaches have been suggested to enhance the generation and diffusion of reactive oxygen species and improve photocatalytic antibacterial performance. Furthermore, this review highlights the practical applications of photocatalysts, underscoring their potential to revolutionize infection control and public health practices.

Although some photocatalytic antimicrobials with visible light activity have been successfully synthesized, most photocatalytic semiconductors are still in the laboratory stage. To further their application in the antimicrobial field, the development of simple and cost-effective synthesis methods that are amenable to mass production is imperative. A comprehensive understanding of the mechanism of photocatalytic sterilization is essential for the design and development of photocatalytic semiconductors. This necessitates the use of advanced in-situ

characterization techniques, theoretical calculations, and molecular dynamics simulations, which collectively contribute to a deeper understanding of the photocatalytic antibacterial mechanisms and effectively guide the synthesis of highly efficient photocatalytic antimicrobials. Moreover, integrating photocatalysis with photothermal and membrane technologies holds significant promise for enhancing the efficacy and applicability of photocatalytic systems. Intergration of photothermal effects can lead to improved solar energy utilization by enabling full-spectrum light absorption, thereby increasing the rates of ROS generation. This approach can address the low energy conversion efficiencies of photocatalytic processes, by leveraging the thermal energy generated alongside chemical reactions, which has been widely studied in photocatalytic environmental governance [85–87]. Additionally, combining membrane technologies with photocatalysis can offer simultaneous disinfection and filtration capabilities, enhancing overall water treatment processes and ensuring the removal of both biological contaminants and particulate matter. Continued innovation in the development of photocatalytic materials is crucial. Strategies such as defect modulation, heterojunction fabrication, and incorporation of thermal storage materials can significantly enhance system performance [88], leading to improved charge separation and light absorption, ultimately resulting in more efficient ROS production. It is essential to develop non-toxic semiconductor photocatalysts that are recyclable, chemically and physically stable, and exhibit good biocompatibility. The recovery of semiconductor photocatalysts in water still presents challenges, leading to reduced disinfection efficiency and impeding the practical application of photocatalytic sterilization. Future research should prioritize the development of easily recyclable photocatalytic films, magnetic photocatalysts, and three-dimensional catalysts to enhance the practical applicability of photocatalytic sterilization.

**Author Contributions:** Literature investigation, conceptualization, and writing—original draft preparation, X.B. and Y.C.; writing—review and editing, B.Z. and R.L.; visualization, investigation J.D.; conceptualization, supervision, H.Y. All authors have read and agreed to the published version of the manuscript.

**Funding:** This work was partly supported by the National Natural Science Foundation of China (22276011, 21607034), Beijing Natural Science Foundation (8192011), the Cultivation Project Funds for Beijing University of Civil Engineering and Architecture (X23042), Science and Technology General Project of Beijing Municipal Education Commission (KM202010016006), the Pyramid Talent Training Project of Beijing University of Civil Engineering and Architecture (JDYC20200313), the Project of Construction and Support for high-level Innovative Teams of Beijing Municipal Institutions (BPHR20220108), the Outstanding Talent Project of Beijing Xicheng District (202323).

**Institutional Review Board Statement:** Not applicable.

**Informed Consent Statement:** Not applicable.

**Data Availability Statement:** Not applicable.

**Conflicts of Interest:** The authors declare no conflict of interest.

## References

1. Redman, C.L.; Jones, N.S. The environmental, social, and health dimensions of urban expansion. *Popul. Environ.* **2005**, *26*, 505–520.
2. Gong, P.; Liang, S.; Carlton, E.J.; Jiang, Q.; Wu, J.; Wang, L.; Remais, J.V. Urbanisation and health in China. *Lancet* **2012**, *379*, 843–852.
3. McMichael, A.J.; Beaglehole, R. The changing global context of public health. *Lancet* **2000**, *356*, 495–499.
4. Parola, P.; Raoult, D. Ticks and tickborne bacterial diseases in humans: An emerging infectious threat. *Clin. Infect. Dis.* **2001**, *32*, 897–928.
5. Amarasiri, M.; Sano, D.; Suzuki, S. Understanding human health risks caused by antibiotic resistant bacteria (ARB) and antibiotic resistance genes (ARG) in water environments: Current knowledge and questions to be answered. *Crit. Rev. Environ. Sci. Technol.* **2020**, *50*, 2016–2059.
6. Singh, S.R.; Krishnamurthy, N.; Mathew, B.B. A review on recent diseases caused by microbes. *J. Appl. Environ. Microbiol.* **2014**, *2*, 106–115.
7. Chen, P.; Guo, X.; Li, F. Antibiotic resistance genes in bioaerosols: Emerging, non-ignorable and pernicious pollutants. *J. Clean. Prod.* **2022**, *348*, 131094.
8. Kohanski, M.A.; Dwyer, D.J.; Collins, J.J. How antibiotics kill bacteria: From targets to networks. *Nat. Rev. Microbiol.* **2010**, *8*, 423–435.
9. Alanis, A.J. Resistance to antibiotics: Are we in the post-antibiotic era? *Arch. Med. Res.* **2005**, *36*, 697–705.
10. Kubacka, A.; Fernandez-Garcia, M.; Colon, G. Advanced nanoarchitectures for solar photocatalytic applications. *Chem. Rev.* **2012**, *112*, 1555–1614.
11. Ahmad, R.; Ahmad, Z.; Khan, A.U.; Mastoi, N.R.; Aslam, M.; Kim, J. Photocatalytic systems as an advanced environmental remediation: Recent developments, limitations and new avenues for applications. *J. Environ. Chem. Eng.* **2016**, *4*, 4143–4164.

12. Yemmireddy, V.K.; Hung, Y.C. Using photocatalyst metal oxides as antimicrobial surface coatings to ensure food safety—Opportunities and challenges. *Compr. Rev. Food Sci. Food Saf.* **2017**, *16*, 617–631.
13. Wang, H.; Li, X.; Zhao, X.; Li, C.; Song, X.; Zhang, P.; Huo, P. A review on heterogeneous photocatalysis for environmental remediation: From semiconductors to modification strategies. *Chin. J. Catal.* **2022**, *43*, 178–214.
14. Fujishima, A.; Honda, K. Electrochemical photolysis of water at a semiconductor electrode. *Nature* **1972**, *238*, 37–38.
15. Nolan, M.; Iwaszuk, A.; Lucid, A.K.; Carey, J.J.; Fronzi, M. Design of novel visible light active photocatalyst materials: Surface modified TiO<sub>2</sub>. *Adv. Mater.* **2016**, *28*, 5425–5446.
16. Qiu, J.; Dai, D.; Yao, J. Tailoring metal–organic frameworks for photocatalytic H<sub>2</sub>O<sub>2</sub> production. *Coord. Chem. Rev.* **2024**, *501*, 215597.
17. Wang, Y.; Liu, M.; Fan, F.; Li, G.; Duan, J.; Li, Y.; Jiang, G.; Yao, W. Enhanced full-spectrum photocatalytic activity of 3D carbon-coated C<sub>3</sub>N<sub>4</sub> nanowires via giant interfacial electric field. *Appl. Catal. B Environ.* **2022**, *318*, 121829.
18. Pang, J.; Mendes, R.G.; Bachmatiuk, A.; Zhao, L.; Ta, H.Q.; Gemming, T.; Liu, H.; Liu, Z.; Rummeli, M.H. Applications of 2D MXenes in energy conversion and storage systems. *Chem. Soc. Rev.* **2019**, *48*, 72–133.
19. Liu, J.; Ma, N.; Wu, W.; He, Q. Recent progress on photocatalytic heterostructures with full solar spectral responses. *Chem. Eng. J.* **2020**, *393*, 124719.
20. Jiao, X.; Zheng, K.; Hu, Z.; Sun, Y.; Xie, Y. Broad-spectral-response photocatalysts for CO<sub>2</sub> reduction. *ACS Cent. Sci.* **2020**, *6*, 653–660.
21. Chen, X.; Cai, Y.; Liang, R.; Tao, Y.; Wang, W.; Zhao, J.; Chen, X.; Li, H.; Zhang, D.J. NH<sub>2</sub>-UiO-66 (Zr) with fast electron transfer routes for breaking down nitric oxide via photocatalysis. *Appl. Catal. B Environ.* **2020**, *267*, 118687.
22. Kipshidze, N.; Yeo, N.; Kipshidze, N. Photodynamic therapy for COVID-19. *Nat. Photonics* **2020**, *14*, 651–652.
23. Constantino, D.S.M.; Dias, M.M.; Silva, A.M.T.; Faria, J.L.; Silva, C.G. Intensification strategies for improving the performance of photocatalytic processes: A review. *J. Clean. Prod.* **2022**, *340*, 130800.
24. Zhang, C.; Li, Y.; Li, M.; Shuai, D.; Zhou, X.; Xiong, X.; Wang, C.; Hu, Q. Continuous photocatalysis via photo-charging and dark-discharging for sustainable environmental remediation: Performance, mechanism, and influencing factors. *J. Hazard. Mater.* **2021**, *420*, 126607.
25. Chen, D.; Cheng, Y.; Zhou, N.; Chen, P.; Wang, Y.; Li, K.; Huo, S.; Cheng, P.; Peng, P.; Zhang, R. Photocatalytic degradation of organic pollutants using TiO<sub>2</sub>-based photocatalysts: A review. *J. Clean. Prod.* **2020**, *268*, 121725.
26. Shi, Y.; Li, M.; Yu, Y.; Zhang, B. Recent advances in nanostructured transition metal phosphides: Synthesis and energy-related applications. *Energy Environ. Sci.* **2020**, *13*, 4564–4582.
27. Nagarajan, S.; Skillen, N.C.; Fina, F.; Zhang, G.; Random, C.; Lawton, L.A.; Irvine, J.T.S.; Robertson, P.K.J. Comparative assessment of visible light and UV active photocatalysts by hydroxyl radical quantification. *J. Photochem. Photobiol. A Chem.* **2017**, *334*, 13–19.
28. Salvador, P. Mechanisms of water photooxidation at n-TiO<sub>2</sub> rutile single crystal oriented electrodes under UV illumination in competition with photocorrosion. *Prog. Surf. Sci.* **2011**, *86*, 41–58.
29. Redza-Dutordoir, M.; Averill-Bates, D.A. Activation of apoptosis signalling pathways by reactive oxygen species. *Biochim. Biophys. Acta (BBA) Mol. Cell Res.* **2016**, *1863*, 2977–2992.
30. Garcia-Diaz, M.; Huang, Y.-Y.; Hamblin, M.R. Use of fluorescent probes for ROS to tease apart Type I and Type II photochemical pathways in photodynamic therapy. *Methods* **2016**, *109*, 158–166.
31. Sasikumar, D.; John, A.T.; Sunny, J.; Hariharan, M. Access to the triplet excited states of organic chromophores. *Chem. Soc. Rev.* **2020**, *49*, 6122–6140.
32. Wang, H.; Jiang, S.; Chen, S.; Li, D.; Zhang, X.; Shao, W.; Sun, X.; Xie, J.; Zhao, Z.; Zhang, Q. Enhanced singlet oxygen generation in oxidized graphitic carbon nitride for organic synthesis. *Adv. Mater.* **2016**, *28*, 6940–6945.
33. Yu, W.; Hu, C.; Bai, L.; Tian, N.; Zhang, Y.; Huang, H.J.N.E. Photocatalytic hydrogen peroxide evolution: What is the most effective strategy? *Nano Energy* **2022**, *104*, 107906.
34. Ollis, D.F. Kinetics of photocatalyzed reactions: Five lessons learned. *Front. Chem.* **2018**, *6*, 378.
35. Nosaka, Y.; Nosaka, A.Y. Generation and Detection of Reactive Oxygen Species in Photocatalysis. *Chem. Rev.* **2017**, *117*, 11302–11336.
36. Winterbourn, C.C. Reconciling the chemistry and biology of reactive oxygen species. *Nat. Chem. Biol.* **2008**, *4*, 278–286.
37. Li, B.; Wang, C.; Li, N.; Liu, T.; Wang, X. Hydrophobic microenvironment mediated photo-Fenton beads confining free radicals in vicinity of water-soluble contaminants for enhancing water purification. *J. Clean. Prod.* **2024**, *434*, 140135.
38. Ma, H.-Y.; Zhao, L.; Guo, L.-H.; Zhang, H.; Chen, F.-J.; Yu, W.-C. Roles of reactive oxygen species (ROS) in the photocatalytic degradation of pentachlorophenol and its main toxic intermediates by TiO<sub>2</sub>/UV. *J. Hazard. Mater.* **2019**, *369*, 719–726.
39. Yan, H.; Wang, R.; Liu, R.; Xu, T.; Sun, J.; Liu, L.; Wang, J. Recyclable and reusable direct Z-scheme heterojunction CeO<sub>2</sub>/TiO<sub>2</sub> nanotube arrays for photocatalytic water disinfection. *Appl. Catal. B Environ.* **2021**, *291*, 120096.
40. Wang, M.; Xu, Z.; Qi, Z.; Cai, Y.; Li, G.; Choi, W.; An, T. Repeated photocatalytic inactivation of E. coli by UV + Ni foam@TiO<sub>2</sub>: Performance and photocatalyst deactivation. *Chem. Eng. J.* **2023**, *468*, 143680.
41. Kumar, S.G.; Rao, K.S.R.K. Comparison of modification strategies towards enhanced charge carrier separation and photocatalytic degradation activity of metal oxide semiconductors (TiO<sub>2</sub>, WO<sub>3</sub> and ZnO). *Appl. Surf. Sci.* **2017**, *391*, 124–148.

42. Dhiman, P.; Rana, G.; Kumar, A.; Sharma, G.; Vo, D.-V.N.; Naushad, M. ZnO-based heterostructures as photocatalysts for hydrogen generation and depollution: A review. *Environ. Chem. Lett.* **2022**, *20*, 1047–1081.
43. Van Dang, H.; Wang, Y.H.; Wu, J.C.S. Z-scheme photocatalyst Pt/GaP-TiO<sub>2</sub>-SiO<sub>2</sub>: Rh for the separated H<sub>2</sub> evolution from photocatalytic seawater splitting. *Appl. Catal. B Environ.* **2021**, *296*, 120339.
44. He, J.; Cheng, J.; Lo, I.M.C. Green photocatalytic disinfection of real sewage: Efficiency evaluation and toxicity assessment of eco-friendly TiO<sub>2</sub>-based magnetic photocatalyst under solar light. *Water Res.* **2021**, *190*, 116705.
45. Huang, J.; Dou, L.; Li, J.; Zhong, J.; Li, M.; Wang, T. Excellent visible light responsive photocatalytic behavior of N-doped TiO<sub>2</sub> toward decontamination of organic pollutants. *J. Hazard. Mater.* **2021**, *403*, 123857.
46. Xiao, B.; Shen, C.; Luo, Z.; Li, D.; Kuang, X.; Wang, D.; Zi, B.; Yan, R.; Lv, T.; Zhou, T.; Zhang, J.; Liu, Q. Cu surface doped TiO<sub>2</sub>: Constructing Cu single-atoms active sites and broadening the photo-response range for efficient photocatalytic hydrogen production. *Chem. Eng. J.* **2023**, *468*, 143650.
47. Chen, Y.; Wang, X.; Zeng, Z.; Lv, M.; Wang, K.; Wang, H.; Tang, X. Towards molecular understanding of surface and interface catalytic engineering in TiO<sub>2</sub>/TiOF<sub>2</sub> nanosheets photocatalytic antibacterial under visible light irradiation. *J. Hazard. Mater.* **2024**, *465*, 133429.
48. Du, M.; Zhao, W.; Ma, R.; Xu, H.; Zhu, Y.; Shan, C.; Liu, K.; Zhuang, J.; Jiao, Z. Visible-light-driven photocatalytic inactivation of *S. aureus* in aqueous environment by hydrophilic zinc oxide (ZnO) nanoparticles based on the interfacial electron transfer in *S. aureus*/ZnO composites. *J. Hazard. Mater.* **2021**, *418*, 126013.
49. Zhu, Z.; Bao, L.; Pestov, D.; Xu, P.; Wang, W.-N. Cellular-level insight into biointerface: From surface charge modulation to boosted photocatalytic oxidative disinfection. *Chem. Eng. J.* **2023**, *453*, 139956.
50. Wang, C.; Liu, D.; Lin, W. Metal–Organic Frameworks as A Tunable Platform for Designing Functional Molecular Materials. *J. Am. Chem. Soc.* **2013**, *135*, 13222–13234.
51. Han, D.; Han, Y.; Li, J.; Liu, X.; Yeung, K.W.K.; Zheng, Y.; Cui, Z.; Yang, X.; Liang, Y. Enhanced photocatalytic activity and photothermal effects of Cu-doped metal-organic frameworks for rapid treatment of bacteria-infected wounds. *Appl. Catal. B Environ. Energy* **2020**, *261*, 118248.
52. Yilmaz, G.; Peh, S.B.; Zhao, D.; Ho, G.W. Atomic-and Molecular-Level Design of Functional Metal–Organic Frameworks (MOFs) and Derivatives for Energy and Environmental Applications. *Adv. Sci.* **2019**, *6*, 1901129.
53. Chen, M.; Zhang, J.; Qi, J.; Dong, R.; Liu, H.; Wu, D.; Shao, H.; Jiang, X. Boronic Acid-Decorated Multivariate Photosensitive Metal–Organic Frameworks for Combating Multi-Drug-Resistant Bacteria. *ACS Nano* **2022**, *16*, 7732–7744.
54. Gogotsi, Y.; Huang, Q. MXenes: Two-Dimensional Building Blocks for Future Materials and Devices. *ACS Nano* **2021**, *15*, 5775–5780.
55. Liu, Z.; Gao, W.; Liu, L.; Luo, S.; Zhang, C.; Yue, T.; Sun, J.; Zhu, M.; Wang, J. Work function mediated interface charge kinetics for boosting photocatalytic water sterilization. *J. Hazard. Mater.* **2023**, *442*, 130036.
56. Friedmann, D.; Mendive, C.; Bahnemann, D. TiO<sub>2</sub> for water treatment: Parameters affecting the kinetics and mechanisms of photocatalysis. *Appl. Catal. B Environ.* **2010**, *99*, 398–406.
57. Lofrano, G.; Ubaldi, F.; Albarano, L.; Carotenuto, M.; Vaiano, V.; Valeriani, F.; Libralato, G.; Gianfranceschi, G.; Fratoddi, I.; Meric, S. Antimicrobial effectiveness of innovative photocatalysts: A review. *Nanomaterials* **2022**, *12*, 2831.
58. Ganguly, P.; Byrne, C.; Breen, A.; Pillai, S.C. Antimicrobial activity of photocatalysts: Fundamentals, mechanisms, kinetics and recent advances. *Appl. Catal. B Environ.* **2018**, *225*, 51–75.
59. Sapińska, D.; Adamek, E.; Masternak, E.; Zielińska-Danch, W.; Baran, W. Influence of pH on the Kinetics and Products of Photocatalytic Degradation of Sulfonamides in Aqueous Solutions. *Toxics* **2022**, *10*, 655.
60. Schwegmann, H.; Ruppert, J.; Frimmel, F.H. Influence of the pH-value on the photocatalytic disinfection of bacteria with TiO<sub>2</sub>—Explanation by DLVO and XDLVO theory. *Water Res.* **2013**, *47*, 1503–1511.
61. Meng, F.; Liu, Y.; Wang, J.; Tan, X.; Sun, H.; Liu, S.; Wang, S. Temperature dependent photocatalysis of g-C<sub>3</sub>N<sub>4</sub>, TiO<sub>2</sub> and ZnO: Differences in photoactive mechanism. *J. Colloid Interface Sci.* **2018**, *532*, 321–330.
62. Chen, Y.-W.; Hsu, Y.-H. Effects of Reaction Temperature on the Photocatalytic Activity of TiO<sub>2</sub> with Pd and Cu Cocatalysts. *Catalysts* **2021**, *11*, 966.
63. Desiati, R.D.; Taspika, M.; Sugiarti, E. Effect of calcination temperature on the antibacterial activity of TiO<sub>2</sub>/Ag nanocomposite. *Mater. Res. Express* **2019**, *6*, 095059.
64. Luan, J.; Shen, Y.; Zhang, L.; Guo, N. Property characterization and photocatalytic activity evaluation of BiGdO<sub>3</sub> nanoparticles under visible light irradiation. *Int. J. Mol. Sci.* **2016**, *17*, 1441.
65. Cai, Y.; Stromme, M.; Welch, K. Photocatalytic antibacterial effects are maintained on resin-based TiO<sub>2</sub> nanocomposites after cessation of UV irradiation. *PLoS ONE* **2013**, *8*, e75929.
66. Yemmireddy, V.K.; Hung, Y.C. Effect of food processing organic matter on photocatalytic bactericidal activity of titanium dioxide (TiO<sub>2</sub>). *Int. J. Food Microbiol.* **2015**, *204*, 75–80.
67. Ng, A.M.; Chan, C.M.; Guo, M.Y.; Leung, Y.H.; Djuricic, A.B.; Hu, X.; Chan, W.K.; Leung, F.C.; Tong, S.Y. Antibacterial and photocatalytic activity of TiO<sub>2</sub> and ZnO nanomaterials in phosphate buffer and saline solution. *Appl. Microbiol. Biotechnol.* **2013**, *97*, 5565–5573.
68. Podporska-Carroll, J.; Myles, A.; Quilty, B.; McCormack, D.E.; Fagan, R.; Hinder, S.J.; Dionysiou, D.D.; Pillai, S.C. Antibacterial properties of F-doped ZnO visible light photocatalyst. *J. Hazard. Mater.* **2017**, *324*, 39–47.

69. He, W.; Kim, H.-K.; Wamer, W.G.; Melka, D.; Callahan, J.H.; Yin, J.-J. Photogenerated Charge Carriers and Reactive Oxygen Species in ZnO/Au Hybrid Nanostructures with Enhanced Photocatalytic and Antibacterial Activity. *J. Am. Chem. Soc.* **2014**, *136*, 750–757.
70. Qin, Y.; Li, H.; Lu, J.; Meng, F.; Ma, C.; Yan, Y.; Meng, M. Nitrogen-doped hydrogenated TiO<sub>2</sub> modified with CdS nanorods with enhanced optical absorption, charge separation and photocatalytic hydrogen evolution. *Chem. Eng. J.* **2020**, *384*, 123275.
71. Jin, Y.; Long, J.; Ma, X.; Zhou, T.; Zhang, Z.; Lin, H.; Long, J.; Wang, X. Synthesis of caged iodine-modified ZnO nanomaterials and study on their visible light photocatalytic antibacterial properties. *Appl. Catal. B Environ.* **2019**, *256*, 117873.
72. Shi, H.; Fan, J.; Zhao, Y.; Hu, X.; Zhang, X.; Tang, Z. Visible light driven CuBi<sub>2</sub>O<sub>4</sub>/Bi<sub>2</sub>MoO<sub>6</sub> p-n heterojunction with enhanced photocatalytic inactivation of E. coli and mechanism insight. *J. Hazard. Mater.* **2020**, *381*, 121006.
73. Jin, C.; Rao, S.; Xie, J.; Sun, Z.; Gao, J.; Li, Y.; Li, B.; Liu, S.; Liu, L.; Liu, Q.; Yang, J. Enhanced photocatalytic antibacterial performance by hierarchical TiO<sub>2</sub>/W<sub>18</sub>O<sub>49</sub> Z-scheme heterojunction with Ti<sub>3</sub>C<sub>2</sub>T<sub>x</sub>-MXene cocatalyst. *Chem. Eng. J.* **2022**, *447*, 137369.
74. Guo, J.; Zhou, J.; Sun, Z.; Wang, M.; Zou, X.; Mao, H.; Yan, F. Enhanced photocatalytic and antibacterial activity of acridinium-grafted g-C<sub>3</sub>N<sub>4</sub> with broad-spectrum light absorption for antimicrobial photocatalytic therapy. *Acta Biomater.* **2022**, *146*, 370–384.
75. Wang, R.; Wu, Z.; Chen, X.; Cheng, B.; Ou, W. Water purification using a BiVO<sub>4</sub>/graphene oxide multifunctional hydrogel based on interfacial adsorption-enrichment and photocatalytic antibacterial activity. *Ceram. Int.* **2023**, *49*, 9657–9671.
76. Izuma, D.S.; Suzuki, N.; Suzuki, T.; Motomura, H.; Ando, S.; Fujishima, A.; Teshima, K.; Terashima, C. A Floatable and Highly Water-Durable TiO<sub>2</sub>-Coated Net for Photocatalytic Antibacterial Water Treatment in Developing Countries. *Water* **2023**, *15*, 320.
77. Yang, H.; He, D.; Liu, C.; Zhou, X.; Qu, J. Magnetic photocatalytic antimicrobial materials for water disinfection. *Sep. Purif. Technol.* **2023**, *325*, 124697.
78. Kumaravel, V.; Nair, K.M.; Mathew, S.; Bartlett, J.; Kennedy, J.E.; Manning, H.G.; Whelan, B.J.; Leyland, N.S.; Pillai, S.C. Antimicrobial TiO<sub>2</sub> nanocomposite coatings for surfaces, dental and orthopaedic implants. *Chem. Eng. J.* **2021**, *416*, 129071.
79. Yao, Y.; Ochiai, T.; Ishiguro, H.; Nakano, R.; Kubota, Y. Antibacterial performance of a novel photocatalytic-coated cordierite foam for use in air cleaners. *Appl. Catal. B Environ.* **2011**, *106*, 592–599.
80. Ubaldi, F.; Valeriani, F.; Volpini, V.; Lofrano, G.; Romano Spica, V. Antimicrobial Activity of Photocatalytic Coatings on Surfaces: A Systematic Review and Meta-Analysis. *Coatings* **2024**, *14*, 92.
81. Qiu, H.; Si, Z.; Luo, Y.; Feng, P.; Wu, X.; Hou, W.; Zhu, Y.; Chan-Park, M.B.; Xu, L.; Huang, D. The mechanisms and the applications of antibacterial polymers in surface modification on medical devices. *Front. Bioeng. Biotechnol.* **2020**, *8*, 910.
82. Zhou, M.; Ou, H.; Li, S.; Qin, X.; Fang, Y.; Lee, S.; Wang, X.; Ho, W. Photocatalytic air purification using functional polymeric carbon nitrides. *Adv. Sci.* **2021**, *8*, 2102376.
83. Li, P.; Li, J.; Feng, X.; Li, J.; Hao, Y.; Zhang, J.; Wang, H.; Yin, A.; Zhou, J.; Ma, X.; Wang, B. Metal-organic frameworks with photocatalytic bactericidal activity for integrated air cleaning. *Nat. Commun.* **2019**, *10*, 2177.
84. Li, J.; Dong, X.; Sun, Y.; Jiang, G.; Chu, Y.; Lee, S.C.; Dong, F. Tailoring the rate-determining step in photocatalysis via localized excess electrons for efficient and safe air cleaning. *Appl. Catal. B Environ.* **2018**, *239*, 187–195.
85. Zhang, J.; Wu, H.; Shi, L.; Wu, Z.; Zhang, S.; Wang, S.; Sun, H. Photocatalysis coupling with membrane technology for sustainable and continuous purification of wastewater. *Sep. Purif. Technol.* **2024**, *329*, 125225.
86. Zhang, J.; Chen, H.; Duan, X.; Sun, H.; Wang, S. Photothermal catalysis: From fundamentals to practical applications. *Mater. Today* **2023**, *68*, 234–253.
87. He, F.; Chen, H.; Li, J.; Zhao, C.; Zhang, J.; Wang, S. Photothermal-mediated advanced oxidation processes for wastewater purification. *Curr. Opin. Chem. Eng.* **2024**, *45*, 101039.
88. He, F.; Lu, Y.; Wu, Y.; Wang, S.; Zhang, Y.; Dong, P.; Wang, Y.; Zhao, C.; Wang, S.; Zhang, J.; Wang, S. Rejoint of Carbon Nitride Fragments into Multi-Interfacial Order-Disorder Homojunction for Robust Photo-Driven Generation of H<sub>2</sub>O<sub>2</sub>. *Adv. Mater.* **2024**, *36*, e2307490.